近海海洋环境科学国家重点实验室（厦门大学）
State Key Laboratory of Marine Environmental Science (Xiamen University)

Optical Oceanography Laboratory

ZhongPing Lee
Xiamen University

Inherent Optical Properties (IOPs)

Lecture 2: Inversion algorithms

Remote-sensing reflectance (sr^{-1}):

$$R_{rs}(\lambda) = \frac{L_w(\lambda, 0^+)}{E_d(\lambda, 0^+)}$$

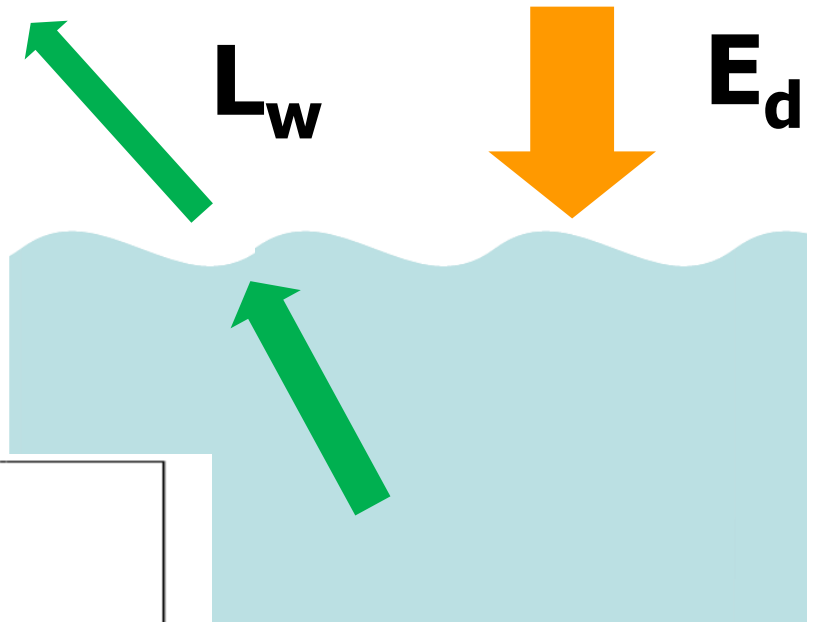

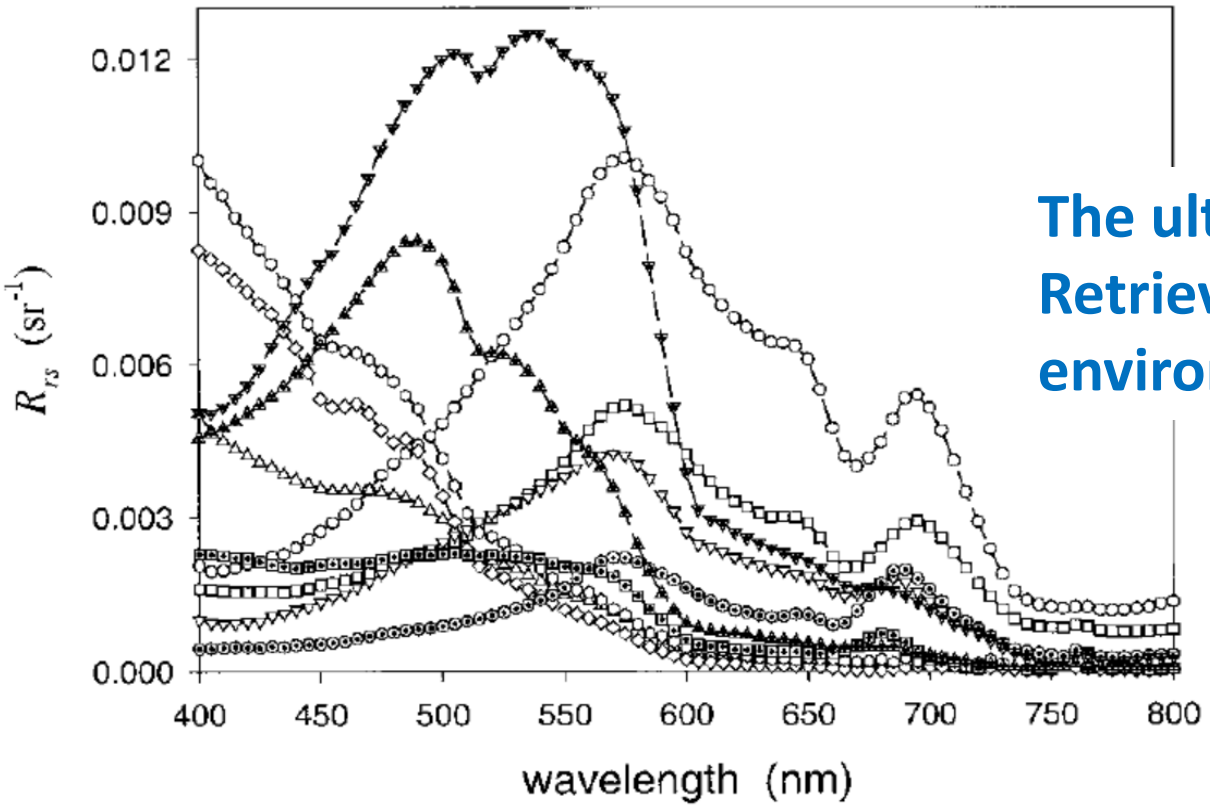

The ultimate objective of RS: Retrieval useful/important environmental information

How?

algorithm!

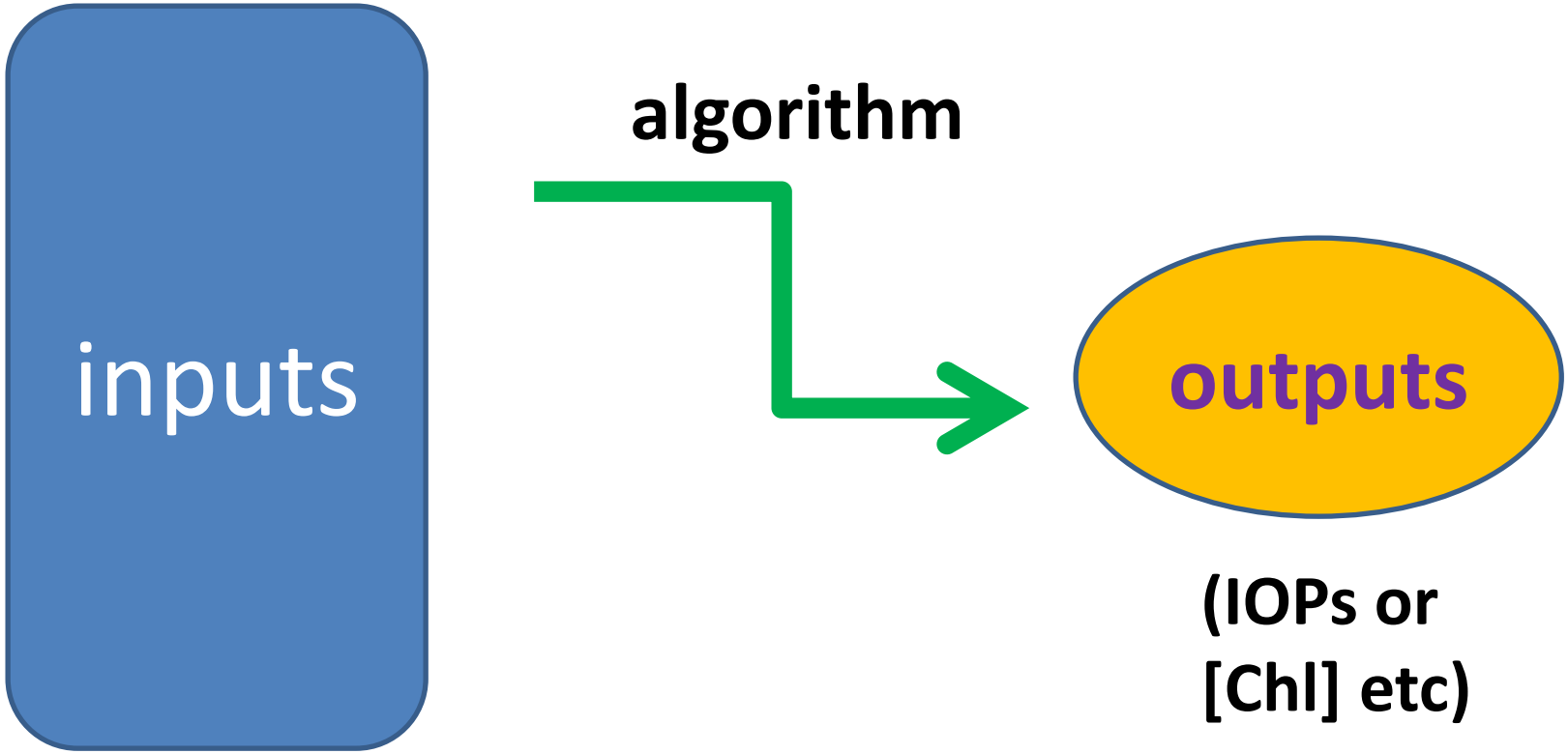
inputs
algorithm
outputs
(IOPs or
[Chl] etc)
(L_w or R_{rs})

Empirical
(explicit or implicit)

Bio-optical models： **No need**

Semi-analytical
(algebraic, LUT, optimization)

Bio-optical models： **Yes**

- **Bottom Up Strategy (BUS)**
- **Top Down Strategy (TDS)**

Chl centered band-ratio algorithms

Algorithm	Type	Result Equation(s)	Band Ratio (R), Coefficients (a)
Global processing (GPs)	power	$C_{13} = 10^{(a0+a1*R1)}$ $C_{23} = 10^{(a2+a3*R2)}$ $[C + P] = C_{13}$; if C_{13} and $C_{23} > 1.5$ μg L^{-1} then $[C + P] = C_{23}$	$R1$ = log(Lwn443/Lwn550) $R2$ = log(Lwn520/Lwn550) a = [0.053, 1.705, 0.522, 2.440]
Clark three-band (C3b)	power	$[C + P] = 10^{(a0+a1*R)}$	R = log((Lwn443 + Lwn520)/Lwn550) a = [0.745, −2.252]
Aiken-C	hyperbolic + power	$C_{21} = \exp(a0 + a1*\ln(R))$ $C_{23} = (R + a2)/(a3 + a4*R)$ $C = C_{21}$; if $C < 2.0$ μg L^{-1} then $C = C_{23}$	R = Lwn490/Lwn555 a = [0.464, −1.989, −5.29, 0.719, −4.23]
Aiken-P	hyperbolic + power	$C_{22} = \exp(a0 + a1*\ln(R))$ $C_{24} = (R + a2)/(a3 + a4*R)$ $[C + P] = C_{22}$; if $[C + P] < 2.0$ μg L^{-1} then $[C + P] = C_{24}$	R = Lwn490/Lwn555 a = [0.696, −2.085, −5.29, 0.592, −3.48]
OCTS-C	power	$C = 10^{(a0+a1*R)}$	R = log((Lwn520 + Lwn565)/Lwn490) a = [0.55006, 3.497]
OCTS-P	multiple regression	$[C + P] = 10^{(a0+a1*R1+a2*R2)}$	$R1$ = log(Lwn443/Lwn520) $R2$ = log(Lwn490/Lwn520) a = [0.19535, −2.079, −3.497]
POLDER	cubic	$C = 10^{(a0+a1*R+a2*R^2+a3*R^3)}$	R = log(Rrs443/Rrs565) a = [0.438, −2.114, 0.916, −0.851]
CalCOFI two-band linear	power	$C = 10^{(a0+a1*R)}$	R = log(Rrs490/Rrs555) a = [0.444, −2.431]
CalCOFI two-band cubic	cubic	$C = 10^{(a0+a1*R+a2*R^2+a3*R^3)}$	R = log(Rrs490/Rrs555) a = [0.450, −2.860, 0.996, −0.3674]
CalCOFI three-band	multiple regression	$C = \exp(a0 + a1*R1 + a2*R2)$	$R1$ = ln(Rrs490/Rrs555) $R2$ = ln(Rrs510/Rrs555) a = [1.025, −1.622, 1.238]
CalCOFI four-band	multiple regression	$C = \exp(a0 + a1*R1 + a2*R2)$	$R1$ = ln(Rrs443/Rrs555) $R2$ = ln(Rrs412/Rrs510) a = [0.753, −2.583, 1.389]
Morel-1	power	$C = 10^{(a0+a1*R)}$	R = log(Rrs443/Rrs555) a = [0.2492, −1.768]
Morel-2	power	$C = \exp(a0 + a1*R)$	R = ln(Rrs490/Rrs555) a = [1.077835, −2.542605]
Morel-3	cubic	$C = 10^{(a0+a1*R+a2*R^2+a3*R^3)}$	R = log(Rrs443/Rrs555) a = [0.20766, −1.82878, 0.75885, −0.73979]
Morel-4	cubic	$C = 10^{(a0+a1*R+a2*R^2+a3*R^3)}$	R = log(Rrs490/Rrs555) a = [1.03117, −2.40134, 0.3219897, −0.291066]

(O'Reilly et al 1998)

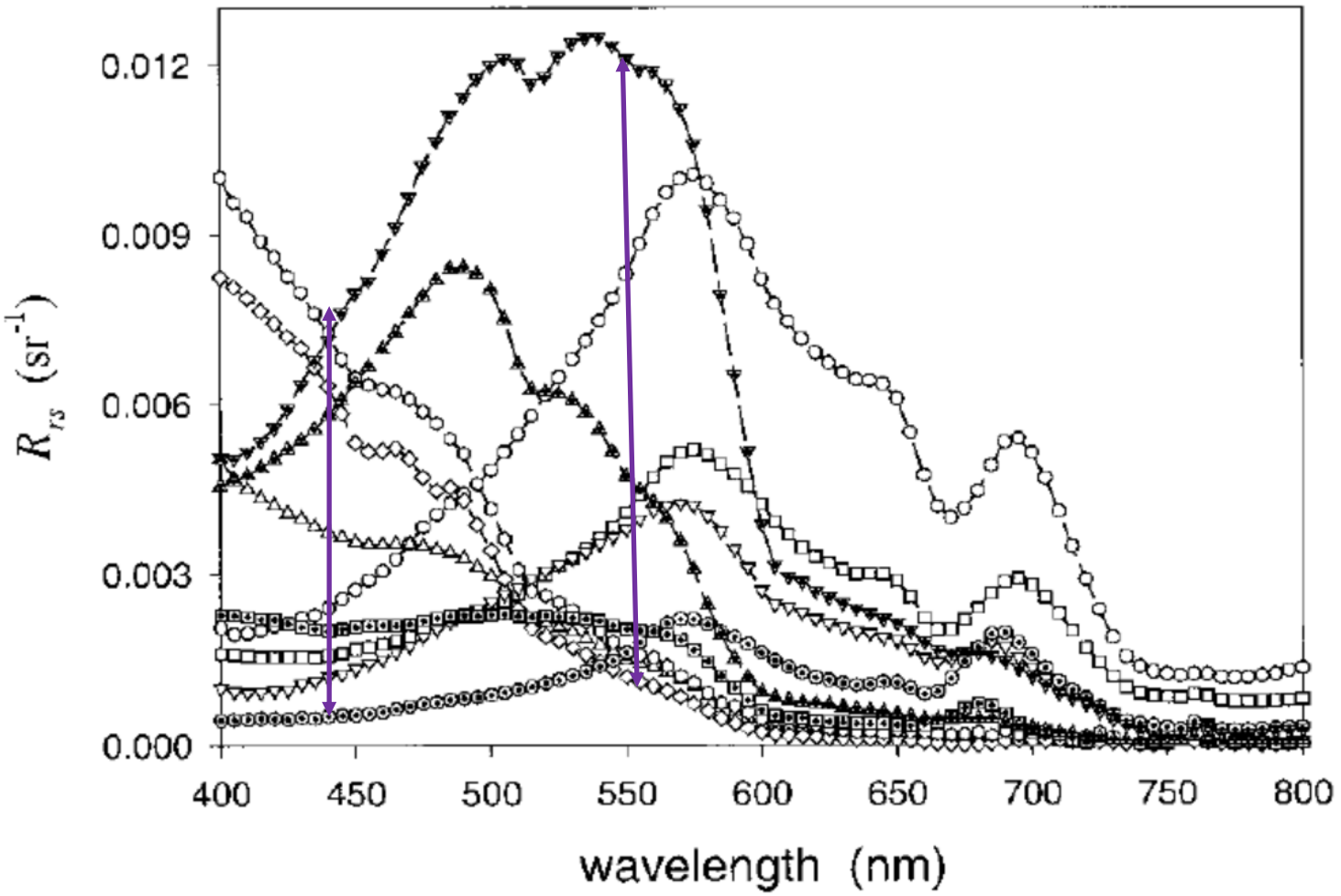
0.012
0.009
0.006
0.003
0.000
R_{rs} (sr^{-1})
400
450
500
550
600
650
700
750
800
wavelength (nm)

Chl based on band difference

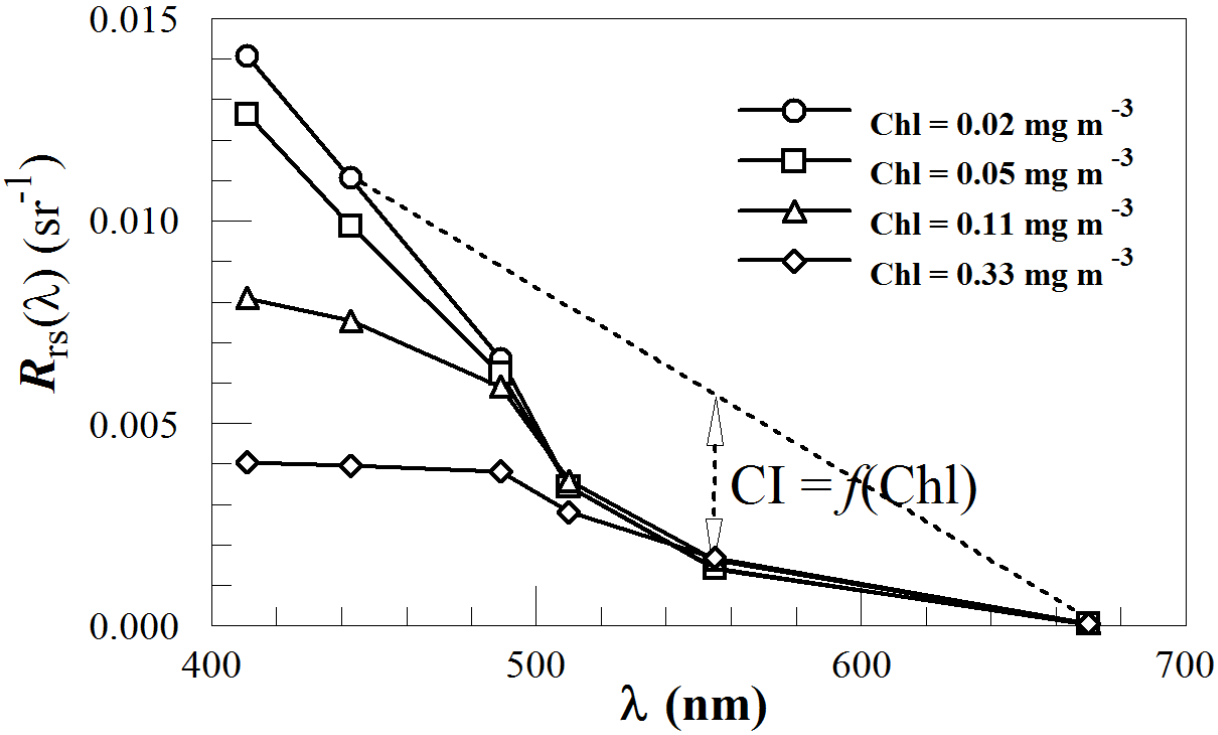

$$CI = R_{rs}(555) - \left\{ R_{rs}(443) + \frac{555-443}{670-443} \times \left[R_{rs}(670) - R_{rs}(443) \right] \right\}$$

$$Chl = 10^{-0.49+191.66CI}; \qquad CI \leq -0.0005 \text{ sr}^{-1}$$

(Hu et al 2012)

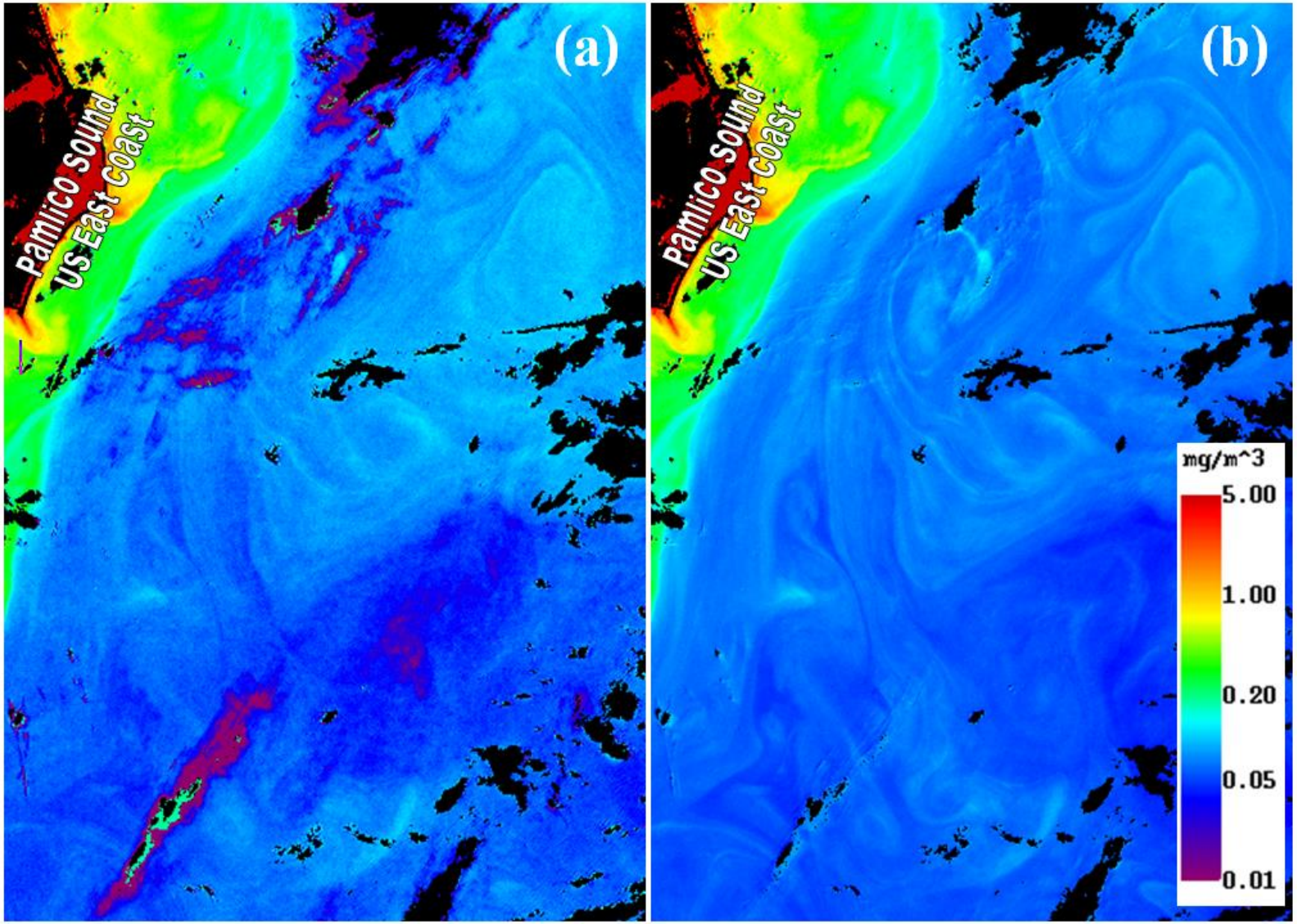
(a)
Pamlico Sound
US East Coast
(b)
Pamlico Sound
US East Coast
mg/m^3
5.00
1.00
0.20
0.05
0.01

(Hu et al 2012)

Empirical:

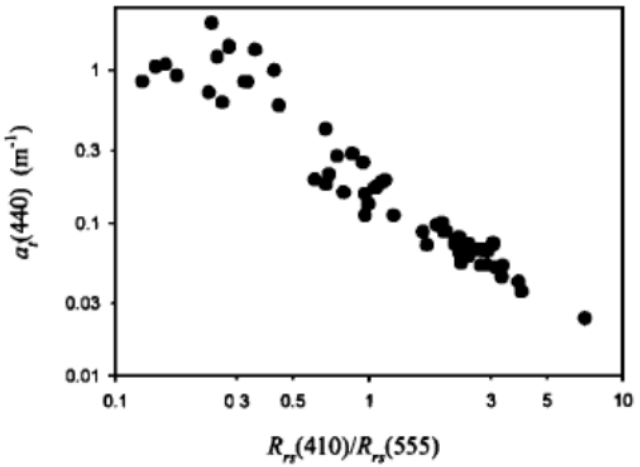

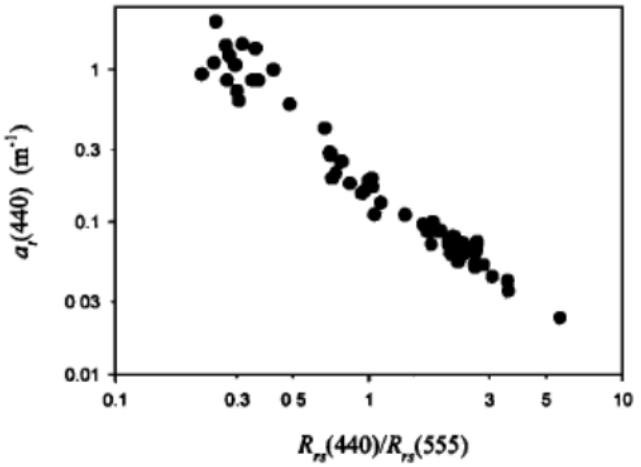

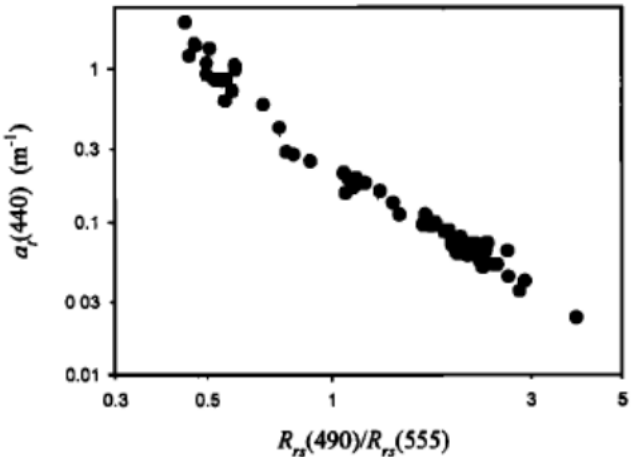

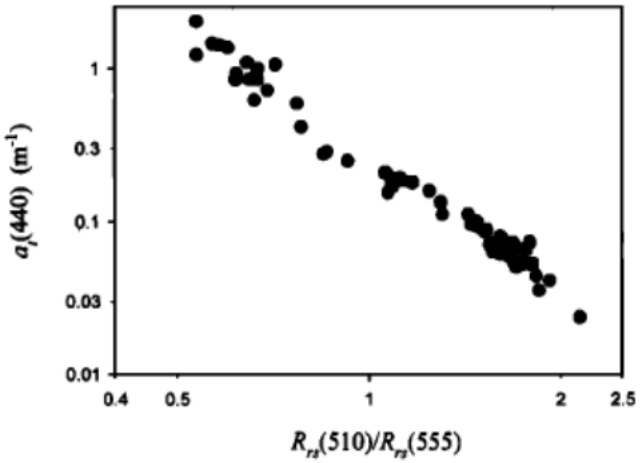

$$a_t(440) = 10^{-0.674-0.531\rho_{25}-0.745\rho_{25}^2-1.469\rho_{35}+2.375\rho_{35}^2}, \quad (14)$$

$$a_\phi(440) = 10^{-0.919+1.037\rho_{25}-0.407\rho_{25}^2-3.531\rho_{35}+1.579\rho_{35}^2}, \quad (20)$$

(Lee et al 1998)

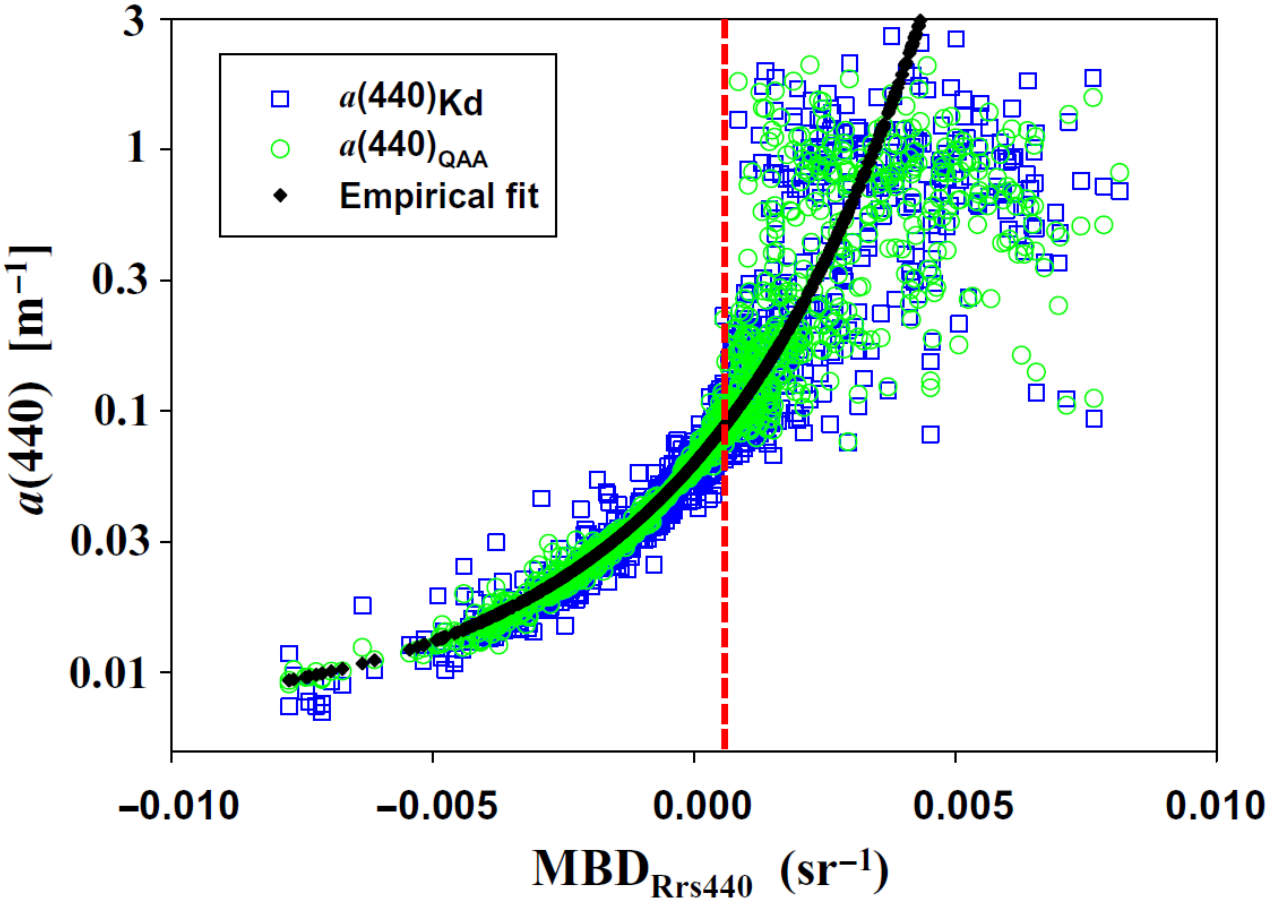

Fig. 3. Relationship between $a(440)$ and MBD_{Rrs440}. The red vertical line indicates the location of $MBD_{Rrs440} = 0.0005\ sr^{-1}$.

$$MBD_{Rrs440} = R_{rs}(555) - \left[R_{rs}(443) + \frac{555-443}{670-443}\left(R_{rs}(670) - R_{rs}(443)\right)\right]$$

(Lee et al., 2023)

$$R_{rs}^{Sat}(\lambda) = R_{rs}(\lambda) + \delta(\lambda) = R_{rs}(\lambda) + y\,\lambda + x$$

$$MBD(R_{rs}^{Sat}) = MBD_{Rrs}$$

Physics-based algorithms (mechanistic)

Remote-sensing reflectance (sr^{-1}):

$$R_{rs}(\lambda) = \frac{L_w(\lambda,0^+)}{E_d(\lambda,0^+)}$$

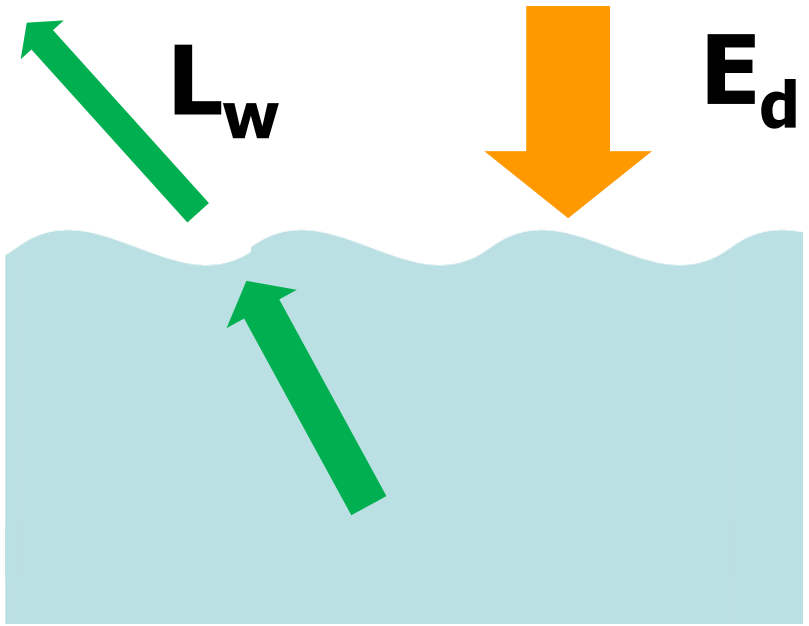

How is R_{rs} related to water's optical (biogeochemical) properties?

Radiative Transfer Equation (inelastic scattering omitted):

$$\frac{d\,L(\Omega)}{d\,l} = -cL(\Omega) + \int L(\Omega')\beta(\Omega',\Omega)\,d\omega$$

$$r_{rs}(\lambda,\Omega) = {L_u(0^-,\Omega)}\Big/{E_d(0^-)}$$

Exact solution (no inelastic scattering):

$$r_{rs}(\lambda,\Omega) \equiv \frac{D_d(\lambda,\theta_S)}{c(\lambda) + k_L(\lambda,\Omega) - f_L(\lambda,\Omega)b_f(\lambda)} \frac{\int_0^{2\pi}\int_0^{\pi/2} \beta(\Omega',\Omega)\ L(\lambda,\Omega')\ \sin(\theta')d\theta' d\phi'}{E_{od}(0^-,\lambda,\theta_S)}$$

(Zaneveld 1995)

$$r_{rs} \cong \frac{1}{\overline{\mu}_d}\frac{\beta(\psi)}{b_b} \Big/ \left[\frac{a}{b_b}\left(1 - \cos(\theta_v)\Psi_{K_{Lu}}\overline{\mu}_\infty{}^{-1}\right) + f_L\left(1 - \widetilde{b}_b{}^{-1}\right) + \widetilde{b}_b{}^{-1}\right], \qquad (12)$$

(Twardowski and Tonizzo, 2018)

Approximations:

Albert and Mobley (2003) :

$$r_{rs}(\lambda,\Omega) = q(\Omega,w)\sum_{i=1}^{4} p_i \left(\frac{b_b(\lambda)}{a(\lambda)+b_b(\lambda)}\right)^i$$

Park and Ruddick (2005)

$$r_{rs}(\lambda,\Omega) = \sum_{i=1}^{4} g_i(\Omega,\nu_b) \left(\frac{b_b(\lambda)}{a(\lambda)+b_b(\lambda)}\right)^i$$

Van Der Woerd and Pasterkamp (2008)

$$\ln[\,r_{rs}(\lambda,\Omega)] = \sum_{i=1}^{4} \sum_{j=1}^{4} P_{ij}(\Omega)[\ln(\,a(\lambda))]^i[\ln(\,b(\lambda))]^j$$

Morel et al (1993, 1996, 2002):

$$r_{rs}(\lambda,\Omega) = g(\lambda, Chl, \Omega)\frac{b_b(\lambda)}{a(\lambda)+b_b(\lambda)}$$

Gordon et al (1988):

$$r_{rs}(\lambda,\pi) = \sum_{i=1}^{2} g_i \left(\frac{b_b(\lambda)}{a(\lambda)+b_b(\lambda)}\right)^i;$$

$$g_1 = 0.0949,\ g_2 = 0.0794$$

Lee et al (2004)

$$r_{rs}(\lambda,\Omega) = g_w(\Omega)\frac{b_{bw}(\lambda)}{a(\lambda)+b_b(\lambda)} + g_p(\lambda,\Omega)\frac{b_{bp}(\lambda)}{a(\lambda)+b_b(\lambda)}$$

$r_{rs} \rightarrow R_{rs}$?

$$R_{rs} = \frac{L_w}{E_d(0^+)}$$

$$E_d(0^-) = t_E E_d(0^+) + \gamma E_u(0^-)$$

$$L_w = \frac{t_L}{n_w^{\,2}} L_u(0^-)$$

(for nadir viewing)

$$R_{rs} = \frac{t_E t_L}{n_w^{\,2}} \frac{r_{rs}}{1 - \gamma R} = \frac{0.52\, r_{rs}}{1 - 1.7\, r_{rs}}$$

Solve Rrs for IOPs or in-water constituents?

Two basic strategies:

1. Bottom-up strategy (BUS):

Assume we know the spectral shapes of the optically active components

2. Top-down strategy (TDS):

Only need the spectral shape information when it is necessary

What are we facing in RS algorithms?

$$R_{rs}(\lambda) = F(a(\lambda), b_b(\lambda))$$

$$R_{rs}(\lambda) = F(a_w(\lambda), a_{ph}(\lambda), a_{dg}(\lambda), b_{bw}(\lambda), b_{bp}(\lambda))$$

$$\begin{cases} R_{rs}(\lambda_1) = F(a_w(\lambda_1), a_{ph}(\lambda_1), a_{dg}(\lambda_1), b_{bw}(\lambda_1), b_{bp}(\lambda_1)) \\ R_{rs}(\lambda_2) = F(a_w(\lambda_2), a_{ph}(\lambda_2), a_{dg}(\lambda_2), b_{bw}(\lambda_2), b_{bp}(\lambda_2)) \\ \vdots \\ R_{rs}(\lambda_n) = F(a_w(\lambda_n), a_{ph}(\lambda_n), a_{dg}(\lambda_n), b_{bw}(\lambda_n), b_{bp}(\lambda_n)) \end{cases}$$

# of unknowns > # of equations.

An ill formulated math problem!

Have to increase # of equations or decrease # of unknowns.

1. Bottom-up strategy (BUS):

Build-up an R_{rs} spectrum block-by-block:

$$a(\lambda) = a_w(\lambda) + \sum a_{xi}(\lambda) \qquad b_b(\lambda) = b_{bw}(\lambda) + \sum b_{bxi}(\lambda)$$

$$a(\lambda) = a_w(\lambda) + a_{ph}(\lambda) + a_d(\lambda) + a_g(\lambda)$$

$$a(\lambda) = a_w(\lambda) + a_{ph}(\lambda) + a_{dg}(\lambda)$$

$$a(\lambda) = a_w(\lambda) + M_1 \left\langle a_{ph}(\lambda) \right\rangle + M_2 \left\langle a_{dg}(\lambda) \right\rangle$$

$$b_b(\lambda) = b_{bw}(\lambda) + b_{bp}(\lambda)$$

$$b_b(\lambda) = b_{bw}(\lambda) + M_3 \left\langle b_{bp}(\lambda) \right\rangle$$

Bio-optical models (forward model)

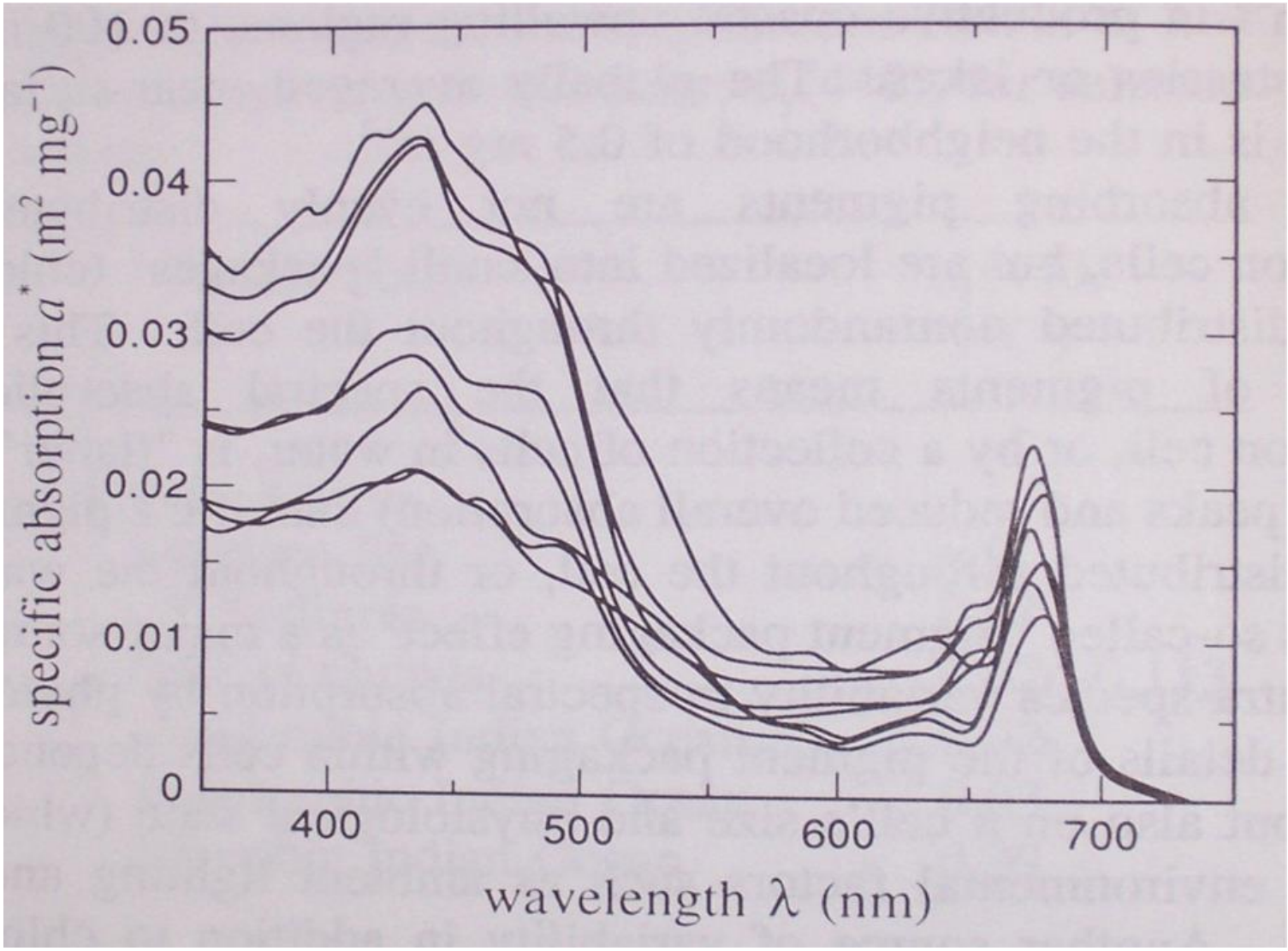

Modeling a_{ph} spectrum

Example of one parameter hyperspectral $a_{ph}(\lambda)$ model:

Bricaud et al (1995):

$$a_{ph}(\lambda) = A_{ph}(\lambda) Chl^{1-B_{ph}(\lambda)}$$

Lee (1994); Lee et al (1998):

$$a_{ph}(\lambda) = \left(a_0(\lambda) + a_1(\lambda)\ln(P)\right)P$$

$$\boldsymbol{P = a_{ph}(440)}$$

Table 2. Spectral Values of the Constants Obtained When Fitting the Variations of $a^*_{ph}(\lambda)$ Versus the (chl a + div a) Concentration (Chl) to Power Laws of the Form $a^*_{ph}(\lambda) = A(\lambda)\,(\mathrm{Chl})^{-B(\lambda)}$ and Determination Coefficients on the Log-Transformed Data r^2

λ, nm	A	B	r^2	λ, nm	A	B
400	0.0263	0.282	0.702	402	0.0271	0.281
404	0.0280	0.282	0.706	406	0.0290	0.281
408	0.0301	0.282	0.710	410	0.0313	0.283
412	0.0323	0.286	0.718	414	0.0333	0.291
416	0.0342	0.293	0.725	418	0.0349	0.296
420	0.0356	0.299	0.733	422	0.0359	0.306
424	0.0362	0.313	0.746	426	0.0369	0.316
428	0.0376	0.317	0.749	430	0.0386	0.314
432	0.0391	0.318	0.750	434	0.0395	0.324
436	0.0399	0.328	0.757	438	0.0401	0.332
440	0.0403	0.332	0.762	442	0.0398	0.339
444	0.0390	0.348	0.774	446	0.0383	0.355
448	0.0375	0.360	0.783	450	0.0371	0.359
452	0.0365	0.362	0.783	454	0.0358	0.366
456	0.0354	0.367	0.789	458	0.0351	0.368
460	0.0350	0.365	0.789	462	0.0347	0.366
464	0.0343	0.368	0.792	466	0.0339	0.369
468	0.0335	0.369	0.793	470	0.0332	0.368
472	0.0325	0.371	0.792	474	0.0318	0.375
476	0.0312	0.378	0.793	478	0.0306	0.379
480	0.0301	0.377	0.791	482	0.0296	0.377
484	0.0290	0.376	0.788	486	0.0285	0.373
488	0.0279	0.369	0.783	490	0.0274	0.361
492	0.0267	0.356	0.774	494	0.0258	0.349
496	0.0249	0.341	0.763	498	0.0240	0.332
500	0.0230	0.321	0.747	502	0.0220	0.311
504	0.0209	0.300	0.722	506	0.0199	0.288
508	0.0189	0.275	0.686	510	0.0180	0.260
512	0.0171	0.249	0.641	514	0.0163	0.237
516	0.0156	0.224	0.578	518	0.0149	0.211
520	0.0143	0.196	0.498	522	0.0137	0.184
524	0.0131	0.173	0.417	526	0.0126	0.162
528	0.0121	0.151	0.332	530	0.0117	0.139
532	0.0113	0.129	0.248	534	0.0108	0.119
536	0.0104	0.109	0.176	538	0.0100	0.100
540	0.0097	0.090	0.116	542	0.0093	0.081

Table 2. Parameters for the Empirical $a_\phi(\lambda)$ Simulation by Eq. (12)[a]

Wavelength	$a_0(\lambda)$	$a_1(\lambda)$
390	0.5813	0.0235
400	0.6843	0.0205
410	0.7782	0.0129
420	0.8637	0.006
430	0.9603	0.002
440	1.0	0
450	0.9634	0.006
460	0.9311	0.0109
470	0.8697	0.0157
480	0.789	0.0152
490	0.7558	0.0256
500	0.7333	0.0559
510	0.6911	0.0865
520	0.6327	0.0981
530	0.5681	0.0969
540	0.5046	0.09
550	0.4262	0.0781
560	0.3433	0.0659
570	0.295	0.06
580	0.2784	0.0581

Example of a two-variable model: (Ciotti et al 2002)

$$a_\phi(\lambda) = a_\phi(505)\{[S_f \cdot \overline{a}_{<pico>}(\lambda)] + [(1 - S_f) \cdot \overline{a}_{<micro>}(\lambda)]\}$$

Table 3. Basis vectors representing the normalized absorption for the smallest ($\overline{a}_{(pico)}(\lambda)$, *Prochlorococcus*) and biggest ($\overline{a}_{(micro)}(\lambda)$, average microplankton) cell sizes in our data set. Wavelength (λ) in nm. Basis vectors for $a^*_{ph}(\lambda)$ can be constructed by setting $\overline{a}_{(pico)}(676)$ to 0.023 $m^2\ mg^{-1}$, $\overline{a}_{(micro)}(674)$ to 0.0086 $m^2\ mg^{-1}$, and scaling for the other wavelengths accordingly.

λ	Pico	Micro	λ	Pico	Micro	λ	Pico	Micro	λ	Pico	Micro	λ	Pico	Micro
400	1.682	1.574												
402	1.734	1.584	462	2.526	1.623	522	0.544	1.013	582	0.111	0.459	642	0.191	0.528
404	1.800	1.600	464	2.455	1.616	524	0.522	0.992	584	0.072	0.452	644	0.174	0.526
406	1.890	1.617	466	2.402	1.606	526	0.486	0.977	586	0.073	0.452	646	0.197	0.528
408	1.978	1.633	468	2.331	1.592	528	0.448	0.959	588	0.073	0.449	648	0.176	0.538
410	2.057	1.654	470	2.281	1.568	530	0.391	0.944	590	0.099	0.443	650	0.168	0.549
412	2.162	1.669	472	2.205	1.542	532	0.375	0.927	592	0.070	0.433	652	0.160	0.574
414	2.269	1.674	474	2.136	1.509	534	0.336	0.909	594	0.095	0.424	654	0.217	0.605
416	2.327	1.684	476	2.063	1.481	536	0.305	0.888	596	0.085	0.416	656	0.244	0.655
418	2.398	1.697	478	2.049	1.459	538	0.292	0.868	598	0.090	0.406	658	0.286	0.720
420	2.457	1.708	480	1.998	1.437	540	0.288	0.847	600	0.086	0.401	660	0.381	0.798
422	2.533	1.710	482	1.930	1.415	542	0.261	0.826	602	0.068	0.400	662	0.437	0.889
424	2.614	1.716	484	1.918	1.399	544	0.245	0.806	604	0.078	0.403	664	0.520	0.979
426	2.663	1.737	486	1.897	1.387	546	0.214	0.785	606	0.069	0.408	666	0.660	1.068
428	2.749	1.763	488	1.867	1.377	548	0.194	0.764	608	0.090	0.416	668	0.716	1.147
430	2.804	1.793	490	1.812	1.367	550	0.187	0.737	610	0.096	0.429	670	0.824	1.207
432	2.840	1.812	492	1.776	1.349	552	0.138	0.711	612	0.094	0.443	672	0.846	1.243
434	2.915	1.827	494	1.701	1.338	554	0.137	0.682	614	0.084	0.458	674	0.816	1.249
436	2.947	1.830	496	1.648	1.319	556	0.111	0.653	616	0.105	0.473	676	0.891	1.227
438	2.978	1.834	498	1.522	1.301	558	0.094	0.626	618	0.128	0.487	678	0.869	1.174
440	3.014	1.824	500	1.439	1.271	560	0.095	0.604	620	0.119	0.495	680	0.812	1.096
442	3.032	1.800	502	1.373	1.242	562	0.070	0.580	622	0.126	0.499	682	0.741	1.004
444	3.011	1.771	504	1.270	1.222	564	0.053	0.555	624	0.138	0.504	684	0.605	0.893

Multiple-parameters model:

$$a_{ph}(\lambda) = \sum_{j=1}^{l} C_j a_j^*(\lambda_{mj}) \exp\left[\frac{(\lambda - \lambda_{mj})^2}{2\sigma_j^2}\right] \qquad (7)$$

TABLE 2. Input Values and Mean Characteristics of Gaussian Bands Reflecting Absorption by Chlorophylls and Carotenoids

Characteristic	Gaussian Band Number and Associated Pigment Species												
	1 chl *a*	2 chl *a*	3 chl *a*	4 chl *c*	5 chl *b*	6 carot.	7 carot.	8 chl *c*	9 chl *a*	10 chl *c*	11 chl *b*	12 chl *a*	13 chl *a*
Input parameters													
Half width, nm	53.8	21.3	32.1	27.2	45.0	45.4	45.9	46.3	35.0	28.9	24.4	21.6	33.5
Center, nm	384	413	435	461	464	490	532	583	623	644	655	676	700
Output parameters													
Half width, nm	43.2	22.7	34.5	29.3	36.0	46.8	49.6	46.8	38.0	24.9	25.4	24.7	29.0
Center, nm	381.5	410.8	433.5	459.2	466.6	487.8	532.0	585.6	620.6	640.7	652.9	675.6	699.8
Specific absorption coefficient, m^2 (mg pigment)$^{-1}$	0.042	0.019	0.047	0.110	0.115	0.035	0.019	0.044	0.005	0.044	0.029	0.021	0.002

Specific absorption coefficients of each pigment are ratios of Gaussian band absorptions (in reciprocal meters) to high-performance liquid chromatography concentrations (in milligrams per cubic meter) of that pigment. Chl, chlorophyll; Carot., carotenoid.

(Hoepffner and Sathyendranath, 1993)

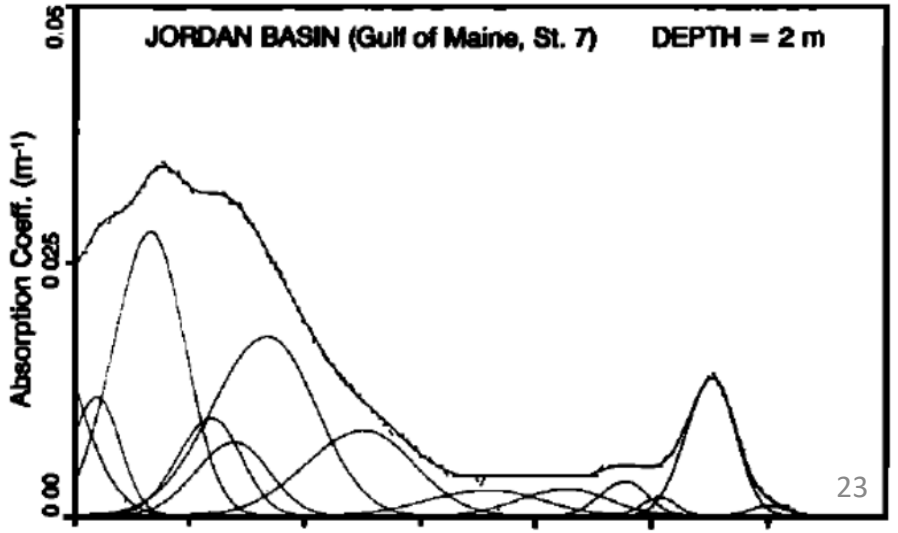

Absorption components: a_{dg} spectrum shapes

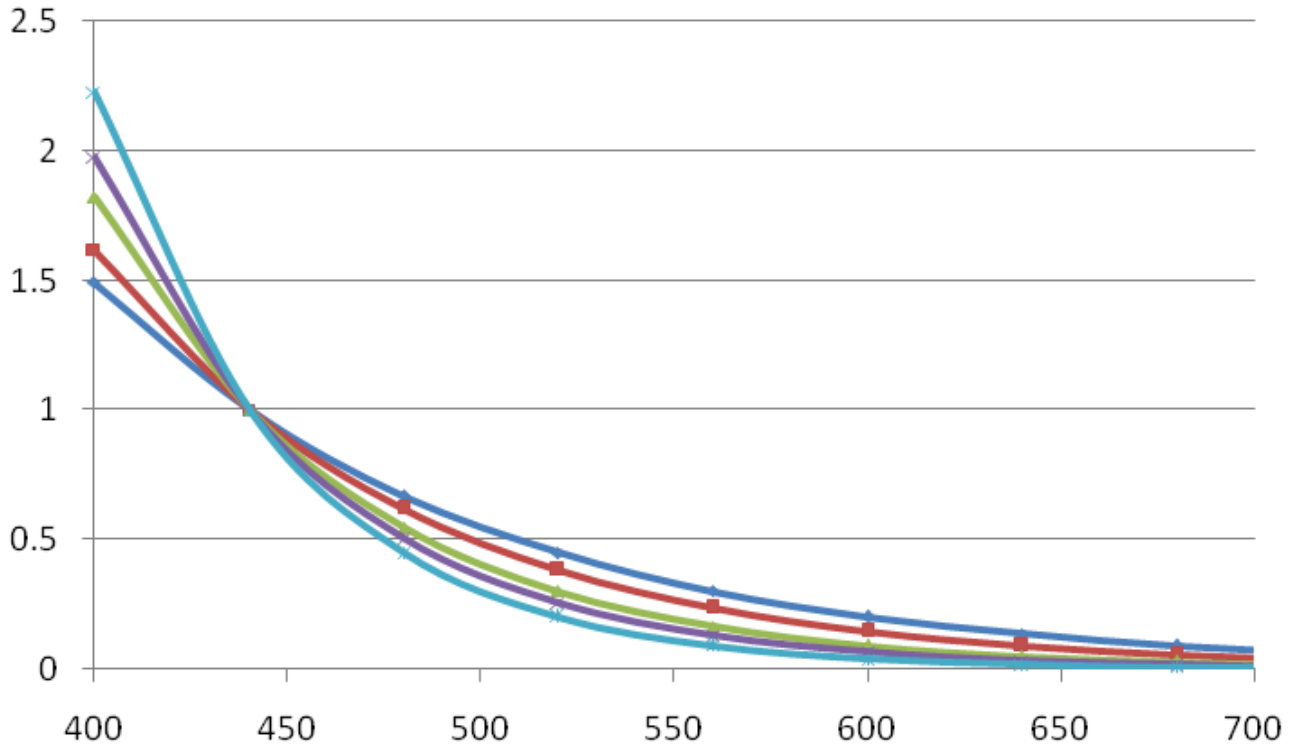

$$\left\langle a_{dg}(\lambda)\right\rangle = e^{-S(\lambda-440)}$$

S: 0.01 – 0.02 nm^{-1}

(*Bricaud et al* 1981)

$$\left\langle b_{bp}(\lambda) \right\rangle = \left(\frac{440}{\lambda} \right)^{\eta}$$

$$R_{rs}(\lambda) = G \frac{b_b(\lambda)}{a(\lambda) + b_b(\lambda)}$$

$$R_{rs}(\lambda) = G\frac{b_{bw}(\lambda) + M_3\langle b_{bp}(\lambda)\rangle}{a_w(\lambda) + M_1\langle a_{ph}(\lambda)\rangle + M_2\langle a_{dg}(\lambda)\rangle + b_{bw}(\lambda) + M_3\langle b_{bp}(\lambda)\rangle}$$

3-variable model to describe an Rrs spectrum

(Sathyendranath et al 1989)

$M_{1\text{-}3}$ are wavelength-independent variables.

Then they could be derived by comparing the modeled Rrs spectrum with the measured Rrs spectrum.

Spectral ranges used for solutions (e.g. examples of BUS):

The **blue-green** domain: e.g., Hoge and Lyon (1996), Carder et al (1999)
The **red-infrared** domain: e.g., Binding et al (2012)
The **entire spectrum** (**spectral optimization**): e.g., Bukata et al (1995), Lee et al (1994,1996,1999), Maritorena et al (2002), Boss and Roesler (2006), Brando et al (2012)， Werdell et al (2013)

Look-Up-Tables (LUT): e.g., Carder et al (1991); Mobley et al (2005)

Spectral Optimization

Matching between measured and modeled R_{rs}

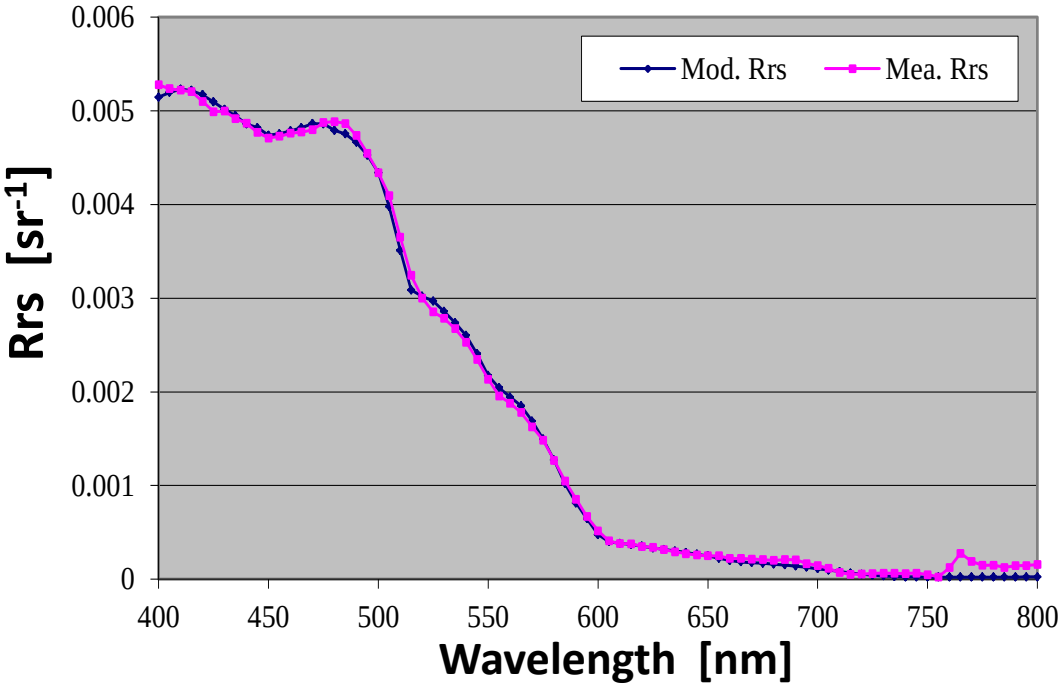

Quantitative measure of the closure (**error function**):

$$\delta_{R_{rs}} = \frac{\sqrt{\Lambda_{\lambda 1}^{\lambda 2}\left(\tilde{R}_{rs}(\lambda) - R_{rs}(\lambda)\right)^2}}{\Lambda_{\lambda 1}^{\lambda 2} R_{rs}(\lambda)} = \sqrt{n}\,\frac{\sqrt{\sum_{\lambda 1}^{\lambda 2}\left(\tilde{R}_{rs}(\lambda) - R_{rs}(\lambda)\right)^2}}{\sum_{\lambda 1}^{\lambda 2} R_{rs}(\lambda)}$$

Logic (assumption) behind SOA:

A unique set of bio-optical properties for each Rrs spectrum.

Algorithms using information in the red-infrared bands

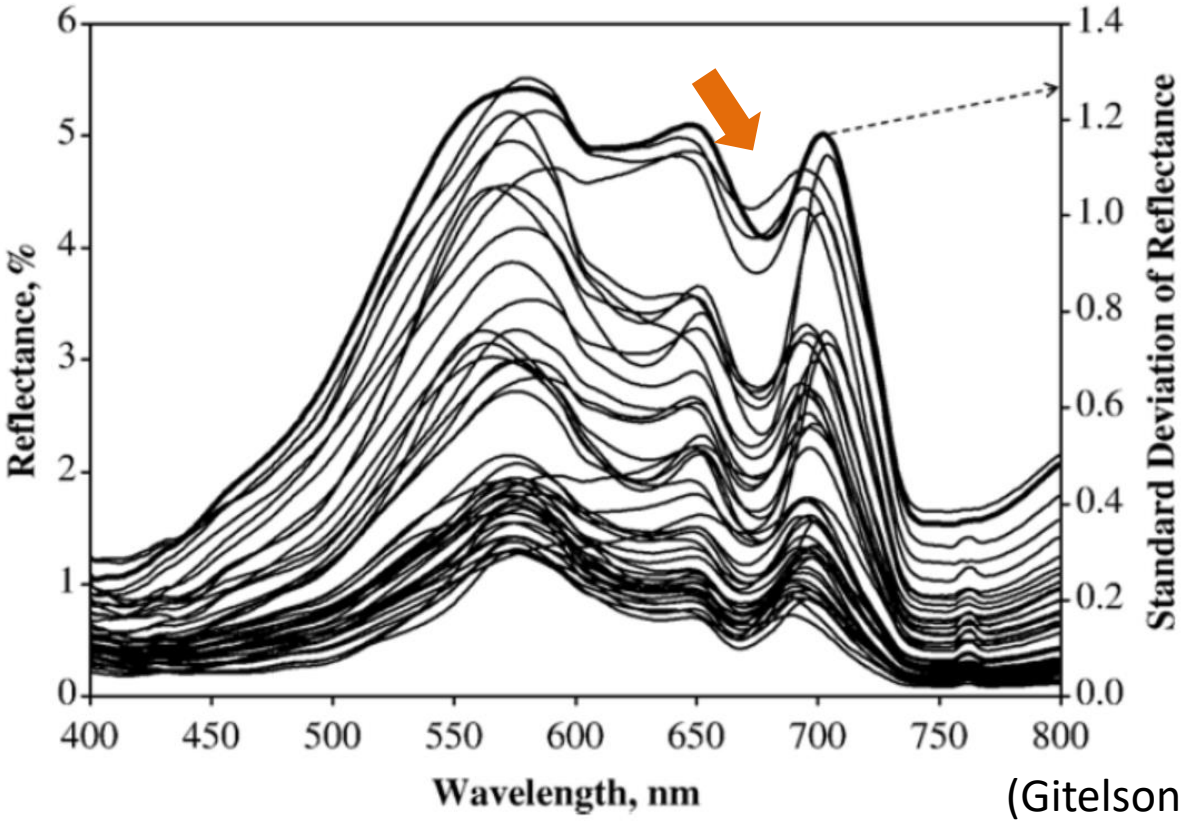

(Gitelson et al 2007)

Two bands

$$Chl = f\left(\frac{Rrs(75x)}{Rrs(67x)}\right)$$

Three bands

$$Chl = f\left(\frac{Rrs(75x)}{Rrs(67x)} - \frac{Rrs(75x)}{Rrs(70x)}\right)$$

$$R_{rs}(\lambda) = G \frac{b_{bw}(\lambda) + M_3 \left\langle b_{bp}(\lambda) \right\rangle}{a_w(\lambda) + M_1 \left\langle a_{ph}(\lambda) \right\rangle + M_2 \left\langle a_{dg}(\lambda) \right\rangle + b_{bw}(\lambda) + M_3 \left\langle b_{bp}(\lambda) \right\rangle}$$

$$R_{rs}(\lambda) \approx G \frac{M_3 \left\langle b_{bp}(\lambda) \right\rangle}{a_w(\lambda) + M_1 \left\langle a_{ph}(\lambda) \right\rangle}$$

$$\frac{R_{rs}(\lambda_{red1})}{R_{rs}(\lambda_{red2})} = \frac{\left\langle b_{bp}(\lambda_{red1}) \right\rangle}{\left\langle b_{bp}(\lambda_{red2}) \right\rangle} \frac{a_w(\lambda_{red2}) + M_1 \left\langle a_{ph}(\lambda_{red2}) \right\rangle}{a_w(\lambda_{red1}) + M_1 \left\langle a_{ph}(\lambda_{red1}) \right\rangle}$$

Proper contrast of Rrs at λ_1 and λ_2 then leads to M_1.

a_{ph}

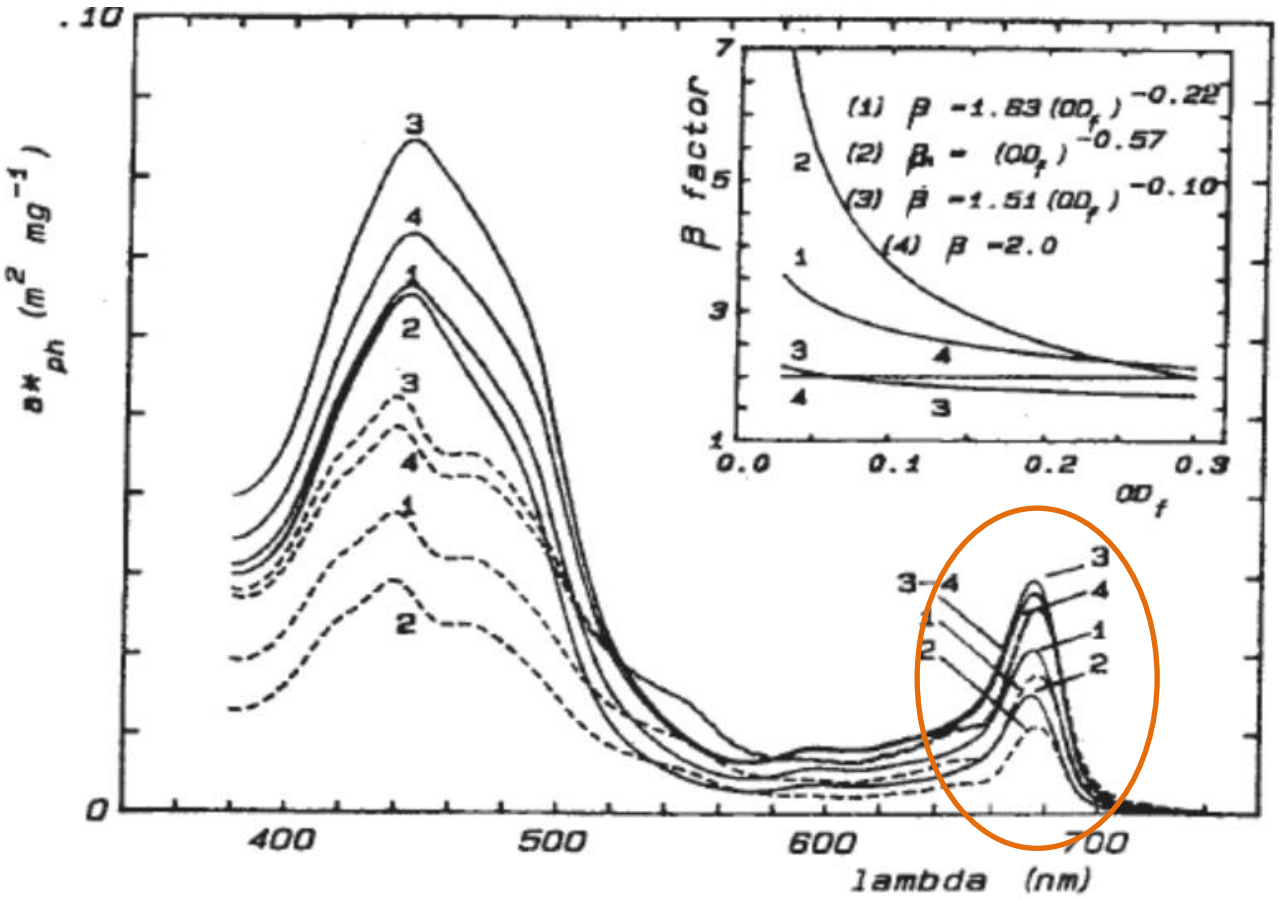
.10
0
a*ph (m2 mg-1)
400
500
600
700
lambda (nm)
β factor
(1) β -1.83 (OD_f)^-0.22
(2) β = (OD_f)^-0.57
(3) β -1.51 (OD_f)^-0.10
(4) β -2.0
0.0
0.1
0.2
0.3
OD_f

2. Top-down strategy (TDS):

$$R_{rs} = G\frac{b_b}{a + b_b}$$

$$R_{rs} \rightarrow b_b \& a \rightarrow a_x$$

Clarity (Secchi depth, light depth, SPM, etc。)

Remote sensing measures the *total* effect:

Water clarity (or turbidity) is also a measure of total effect.

Examples of TDS:

Loisel & Stramski (2000), QAA (Lee et al, 2002); Smyth et al (2006); Doran et al (2007).

The Quasi-Analytical Algorithm (QAA)

Forward modeling:

(a, b_b, etc) → Rrs

$$R_{rs} \approx 0.05 \frac{b_b}{a + b_b}$$

QAA:

(a, b_b) ← Rrs

The data flow of QAA:

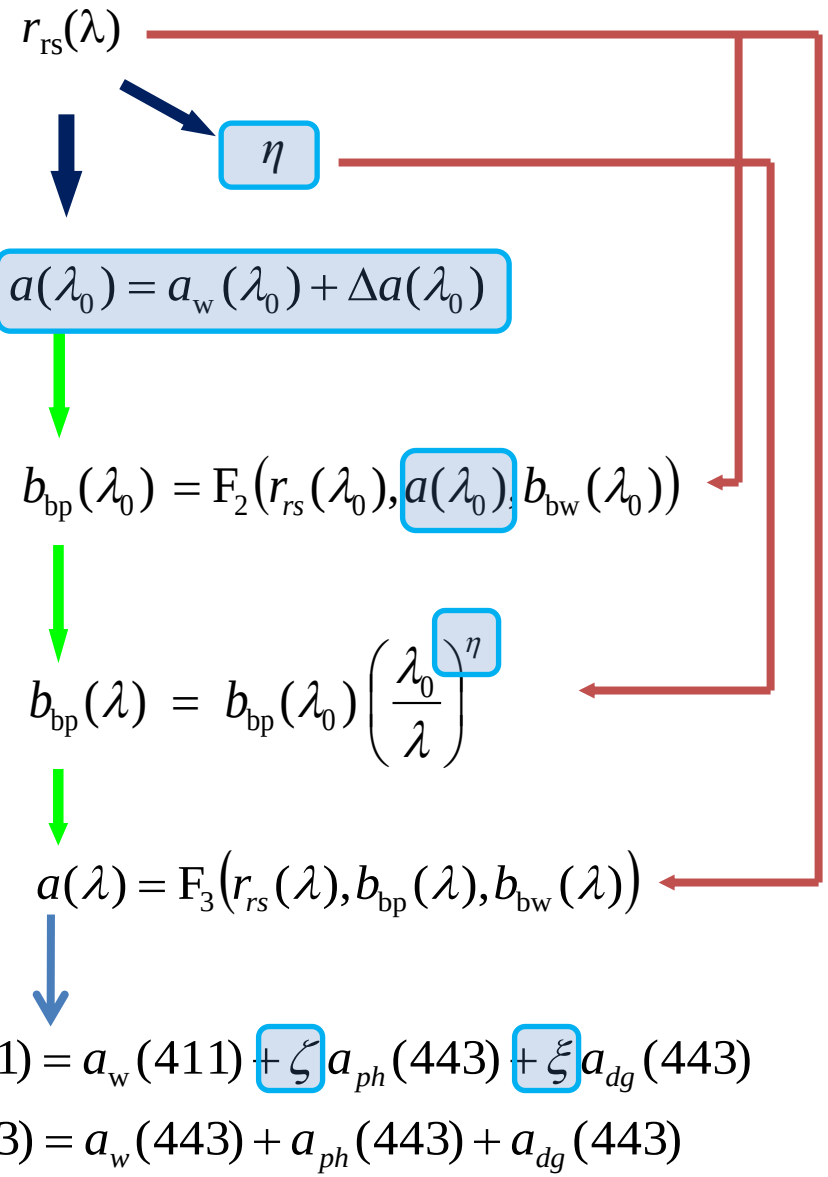

$$\zeta = \frac{a_{ph}(411)}{a_{ph}(443)}$$

$$\xi = \frac{a_{dg}(411)}{a_{dg}(443)}$$

(Lee et al 2002)

Logic behind QAA (and its updated versions):

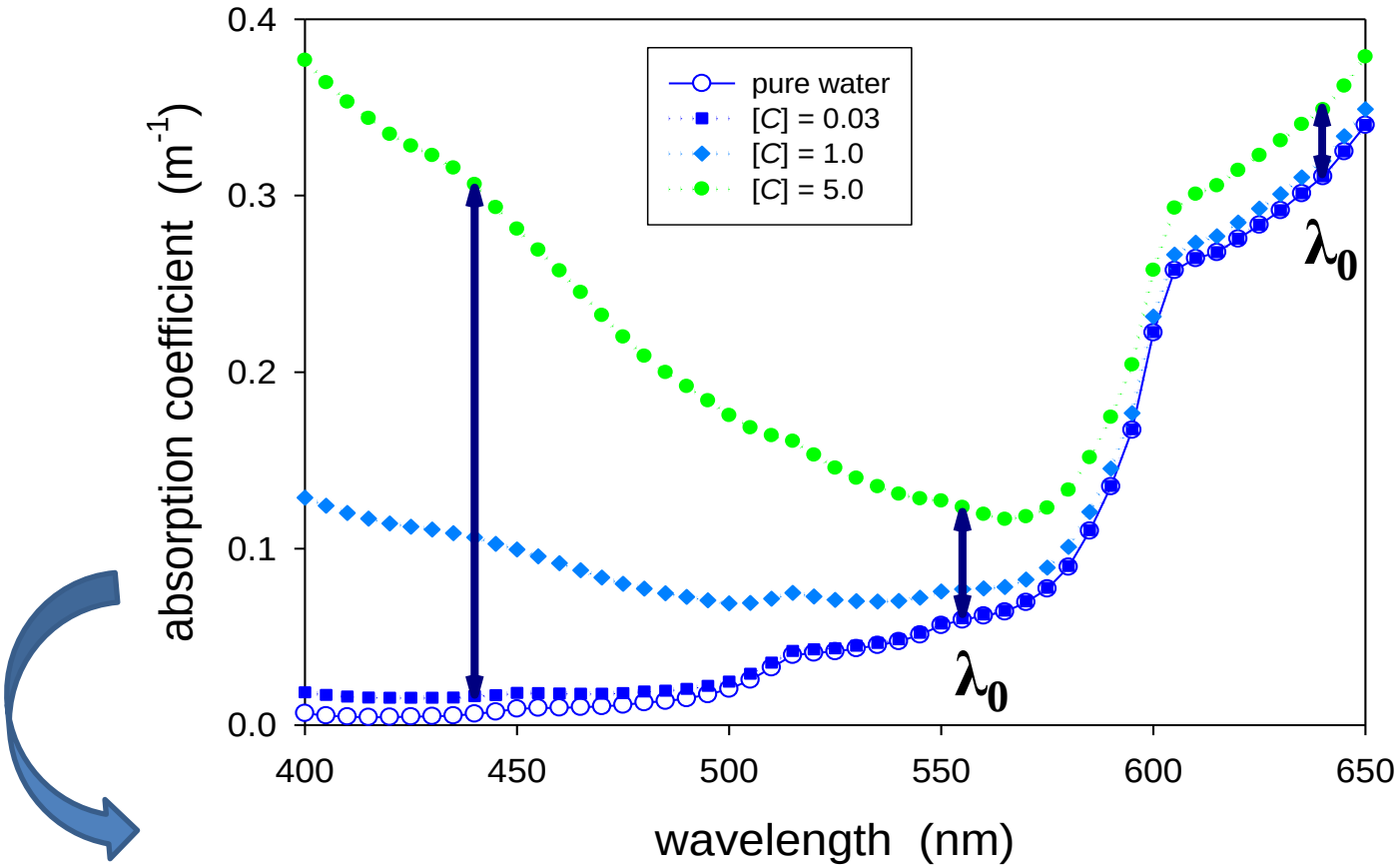

For a reference wavelength, λ_0, variation of $a(\lambda_0)$ is limited.

Known $a(\lambda_0)$, enables calculation of $b_b(\lambda_0)$ from $R_{rs}(\lambda_0)$; propagate $b_b(\lambda_0)$ to $b_b(\lambda)$, then enables calculation of $a(\lambda)$ from $R_{rs}(\lambda)$.

No need of spectral model of $a_x(\lambda)$ in this process.

When 550 nm as the reference wavelength (λ_0)

$$a(550) = a_w(550) + 10^{-1.146 - 1.366\chi - 0.469\chi^2}$$

$$\chi = \log\left(\frac{r_{rs}(443) + r_{rs}(490)}{r_{rs}(\lambda_0) + 5\frac{r_{rs}(667)}{r_{rs}(490)} r_{rs}(667)}\right)$$

$a_w(550) = 0.0565$

Empirical!

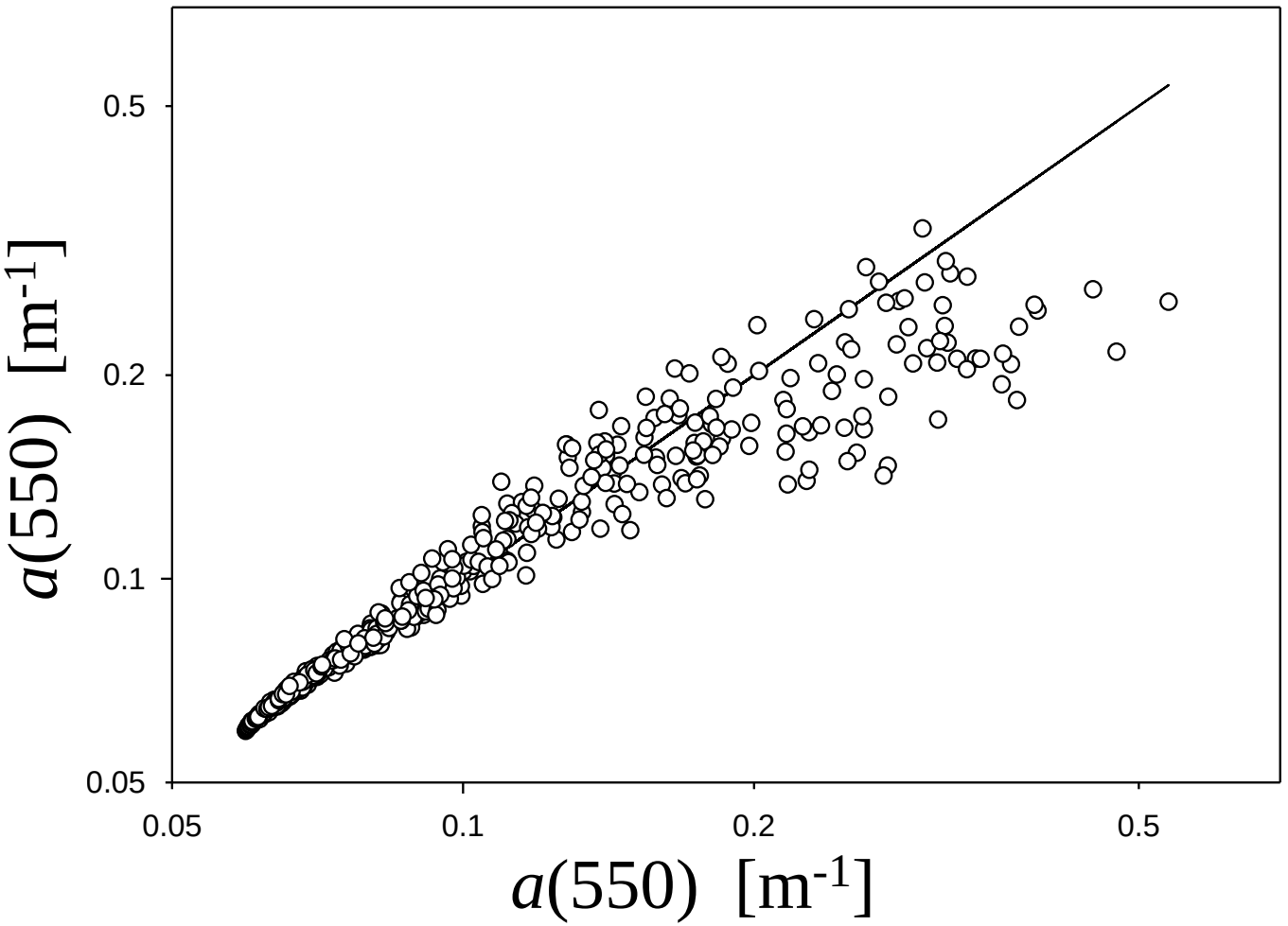
0.5
0.2
0.1
0.05
0.05
0.1
0.2
0.5
a(550) [m-1]
a(550) [m-1]

Invert Rrs:

$R_{rs} \Rightarrow r_{rs} \Rightarrow \{a \& b_b\}$

$r_{rs}(\lambda) = R_{rs}(\lambda)/(0.52 + 1.7\, R_{rs}(\lambda))$

$$r_{rs} = g_0\left(\frac{b_b}{a+b_b}\right) + g_1\left(\frac{b_b}{a+b_b}\right)^2$$

g_0=0.089,g_1=0.125

$$u(\lambda) = \frac{b_b(\lambda)}{a(\lambda)+b_b(\lambda)} = \frac{-g_0 + \sqrt{(g_0)^2 + 4\,g_1 * r_{rs}(\lambda)}}{2g_1}$$

$$a(550) = a_w(550) + 10^{-1.146 - 1.366\chi - 0.469\chi^2}$$

$$b_{bp}(550) = \frac{u(550)\, a(550)}{1 - u(550)} - b_{bw}(550)$$

$$b_{bp}(\lambda) = b_{bp}(550)\left(\frac{550}{\lambda}\right)^{\eta}$$

Empirical:

$$\eta = 2.0\left(1 - 1.2\ \exp\left(-0.9\frac{r_{rs}(443)}{r_{rs}(55x)}\right)\right)$$

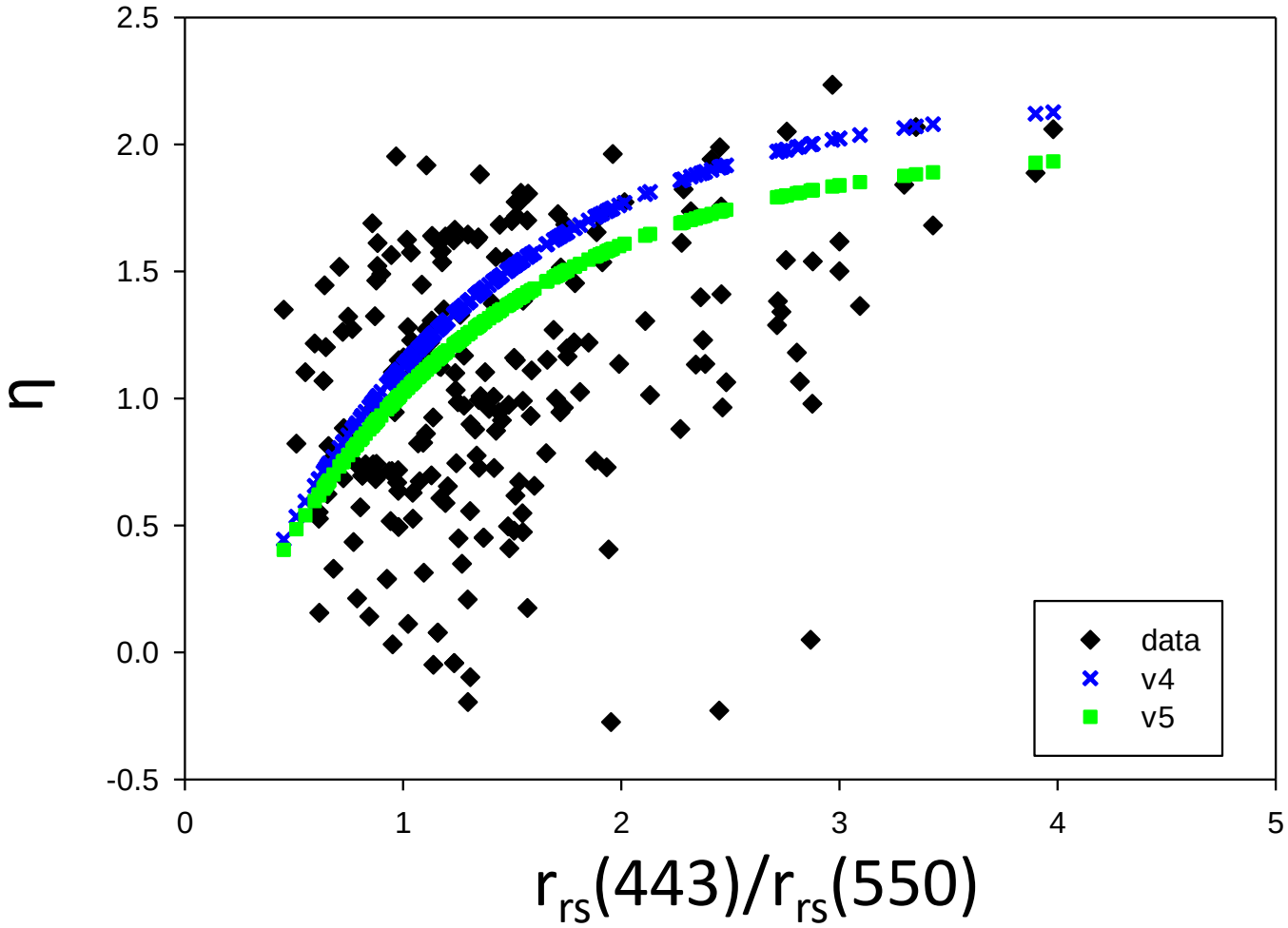

$$b_b(\lambda) = b_{bw}(\lambda) + b_{bp}(\lambda)$$

$$a(\lambda) = \frac{(1-u(\lambda))\, b_b(\lambda)}{u(\lambda)}$$

$$a(\lambda) = a_w(\lambda) + a_{ph}(\lambda) + a_{dg}(\lambda)$$

$$\begin{cases} a(410) = a_w(410) + a_{ph}(410) + a_{dg}(410), \\ a(440) = a_w(440) + a_{ph}(440) + a_{dg}(440). \end{cases}$$

$$\zeta = \frac{a_{ph}(410)}{a_{ph}(440)} \qquad \xi = \frac{a_{dg}(410)}{a_{dg}(440)}$$

$$\begin{cases} a(410) = a_w(410) + \zeta\, a_{ph}(440) + \xi\, a_{dg}(440), \\ a(440) = a_w(440) + a_{ph}(440) + a_{dg}(440). \end{cases}$$

$$\begin{cases} a(410) = a_w(410) + \zeta\, a_{ph}(440) + \xi\, a_{dg}(440), \\ a(440) = a_w(440) + a_{ph}(440) + a_{dg}(440). \end{cases}$$

$$\begin{cases} a_g(440) = \dfrac{\big(a(410) - \zeta\, a(440)\big) - \big(a_w(410) - \zeta\, a_w(440)\big)}{\xi - \zeta}, \\ a_{ph}(440) = a(440) - a_w(440) - a_{dg}(440). \end{cases}$$

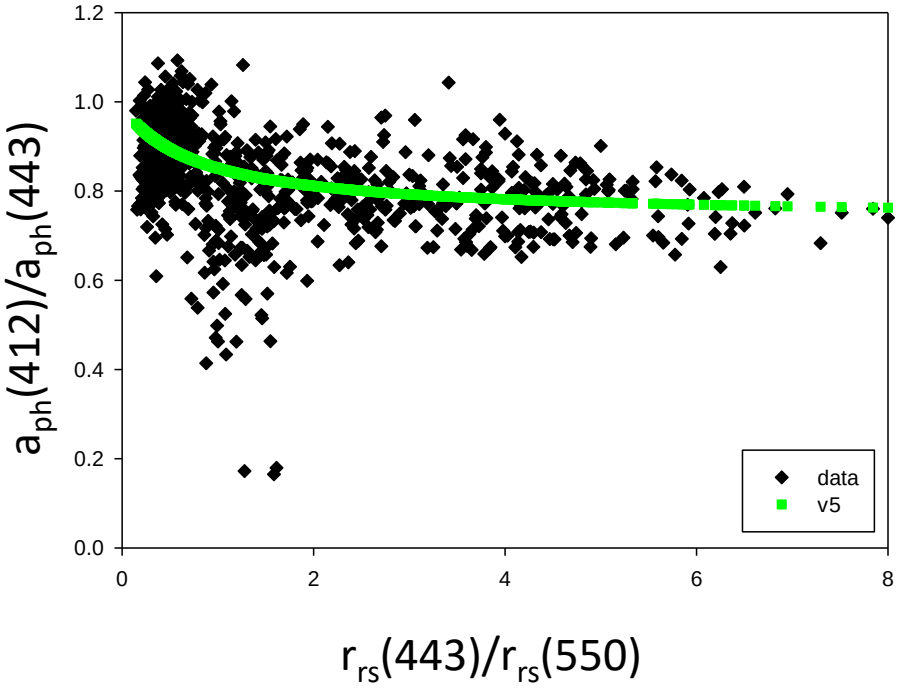

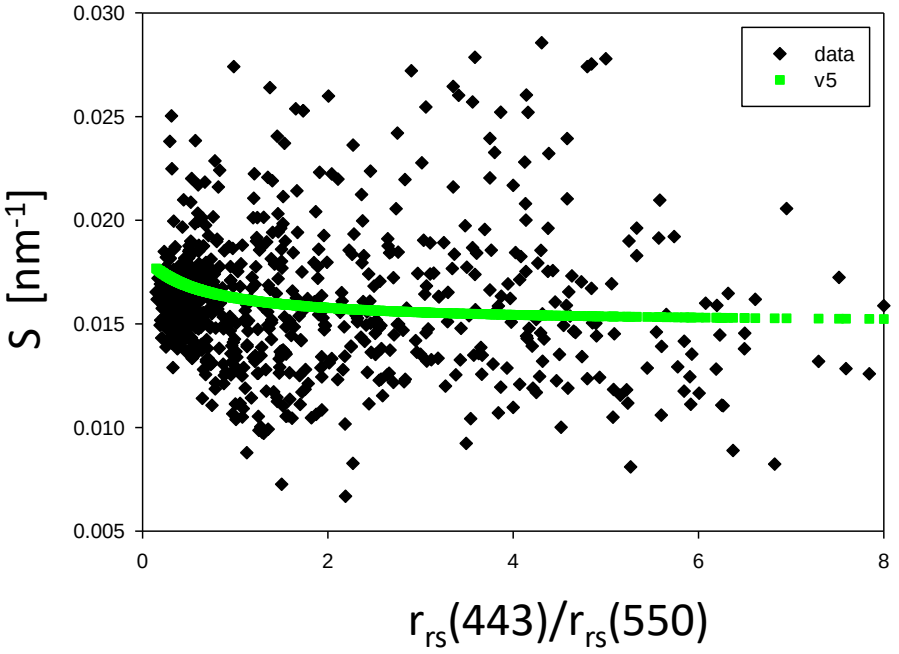

$$\zeta = 0.74 + \frac{0.2}{0.8 + r_{rs}(443)/r_{rs}(550)}$$

$$\xi = e^{S(443-411)},$$

$$S = 0.015 + \frac{0.002}{0.6 + r_{rs}(443)/r_{rs}(550)}$$

Empirical!

Ensemble solutions:

Wang et al. 2005; Zheng et al. 2015

$$a(\lambda) = a_w(\lambda) + \mathrm{M}_1 \left\langle a_{ph}(\lambda) \right\rangle + M_2 \left\langle a_{dg}(\lambda) \right\rangle$$

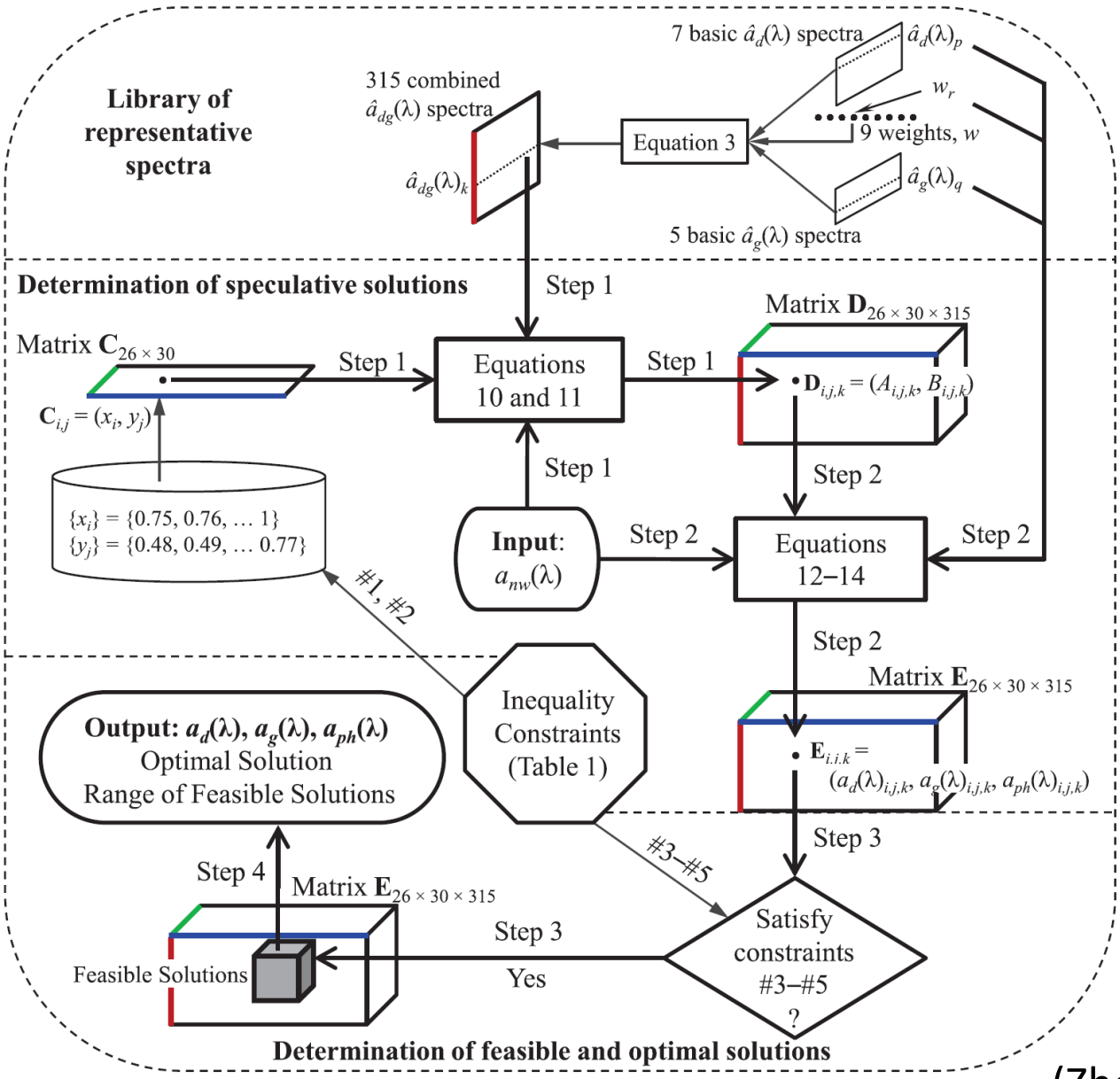

(Zheng et al. 2015)

What is band-ratio derived [Chl]?

$$[Chl] = f_1\left(R_{rs}(\lambda_i)/R_{rs}(\lambda_j)\right)$$

$$R_{rs}(\lambda_i)/R_{rs}(\lambda_j) = f_2\left(\frac{b_{bw}(\lambda_i)+b_{bp}(\lambda_i)}{b_{bw}(\lambda_j)+b_{bp}(\lambda_j)}\frac{a_w(\lambda_j)+a_{ph}(\lambda_j)+a_{dg}(\lambda_j)}{a_w(\lambda_i)+a_{ph}(\lambda_i)+a_{dg}(\lambda_i)}\right)$$

[Chl] is actually an IOP product

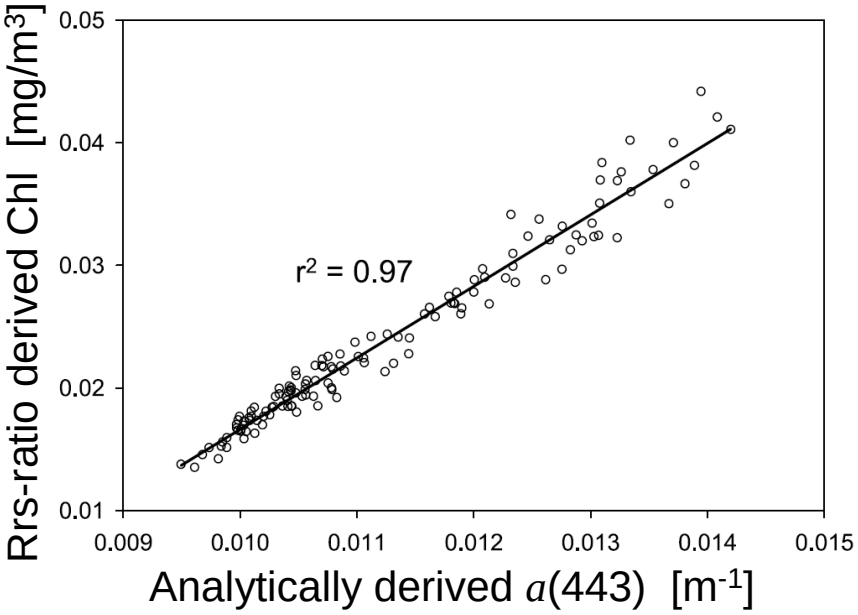

At the center of South Pacific Gyre

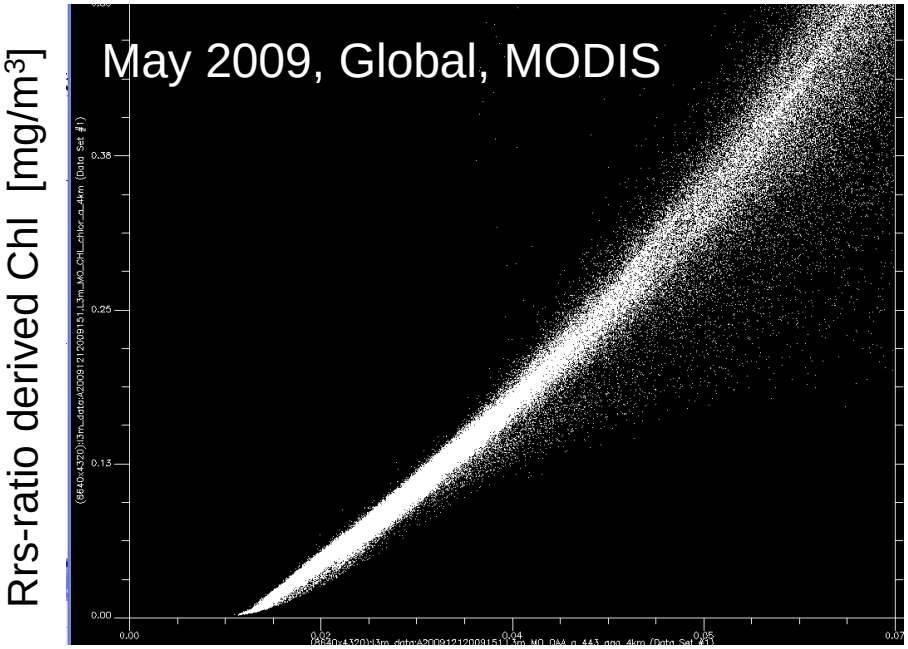

Ratio-derived “Chl” is re-scaled total absorption coefficient.

Correction of Raman-Scattering contribution:

$$R_{rs}^{T}(\lambda) = R_{rs-E}(\lambda) + R_{rs-Ram}(\lambda)$$

$$R_{rs-Ram}(\lambda) = \frac{t^2}{n^2}\frac{\tilde{\beta}^r(\theta_s \to \pi) b_r(\lambda_{\mathrm{em}}) E_d(0^+, \lambda_{\mathrm{ex}})}{(K_d(\lambda_{\mathrm{ex}}) + \kappa_L(\lambda_{\mathrm{em}})) E_d(0^+, \lambda_{\mathrm{em}})} \times \left[1 + \frac{b_b(\lambda_{\mathrm{ex}})}{\mu_u(K_d(\lambda_{\mathrm{ex}}) + \kappa(\lambda_{\mathrm{ex}}))} + \frac{b_b(\lambda_{\mathrm{em}})}{2\mu_u \kappa(\lambda_{\mathrm{em}})}\right]. \quad (7)$$

(Mobley 2012, Westberry et al 2013)

Solve for $R_{rs\text{-}Ram}$ and IOPs through iteration

Empirical scheme:

$$R_{rs-E}(\lambda) = \frac{R_{rs}^{T}(\lambda)}{1 + RF(\lambda)}$$

$$RF(\lambda) = \alpha(\lambda)\left(\frac{R_{rs}^{T}(440)}{R_{rs}^{T}(550)}\right) + \beta_1(\lambda)\left(R_{rs}^{T}(550)\right)^{\beta_2(\lambda)}.$$

(Lee et al 2013)

RF: Raman factor

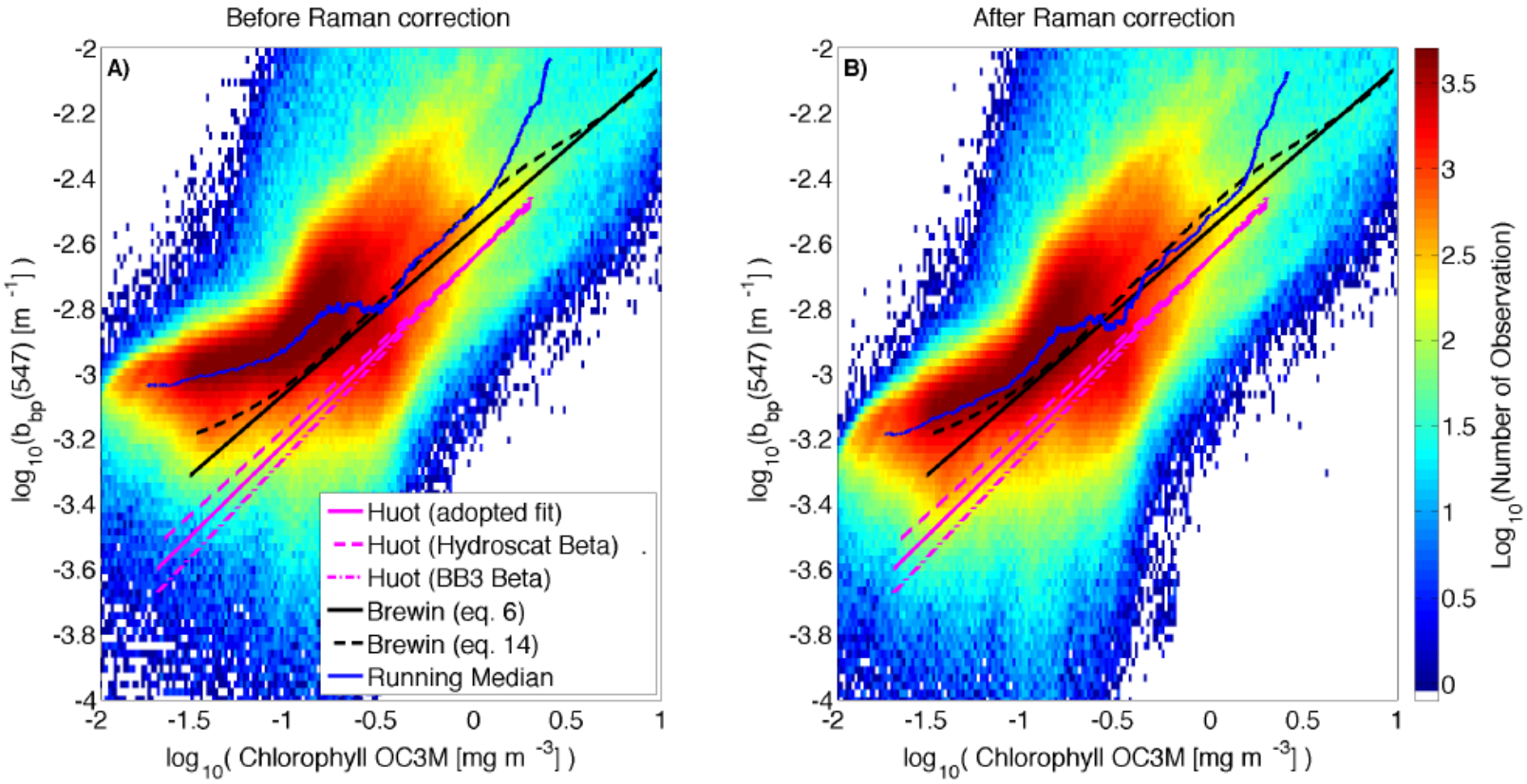

(Lee and Huot, 2014)

Impact of Sensor Specifics on RS products

Sensor Specifics:

Spectral: Number of bands; Position of bands; Width of bands

Signal-to-noise: SNR

Pixel size: Spatial resolution

Revisit: Temporal resolution

How these designs affect remote sensing products?

a) Inversion vs number of spectral bands:

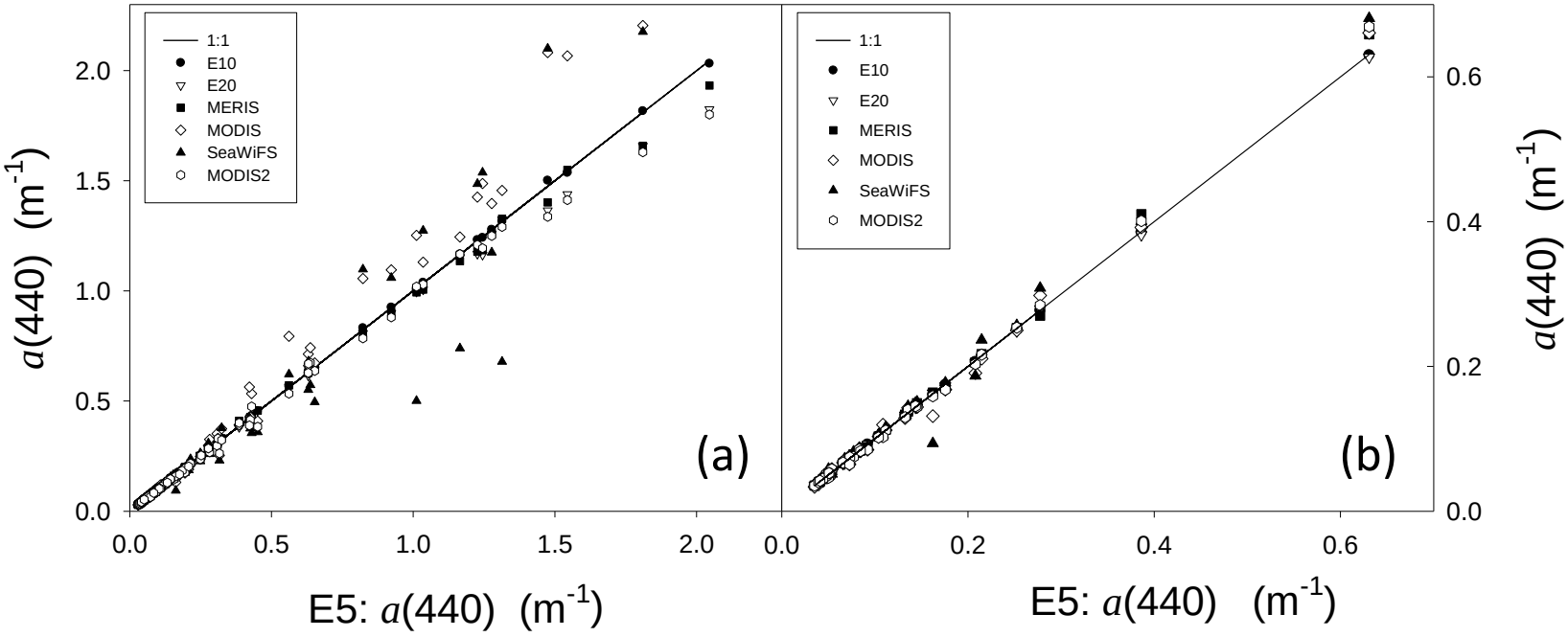

(Lee and Carder 2002)

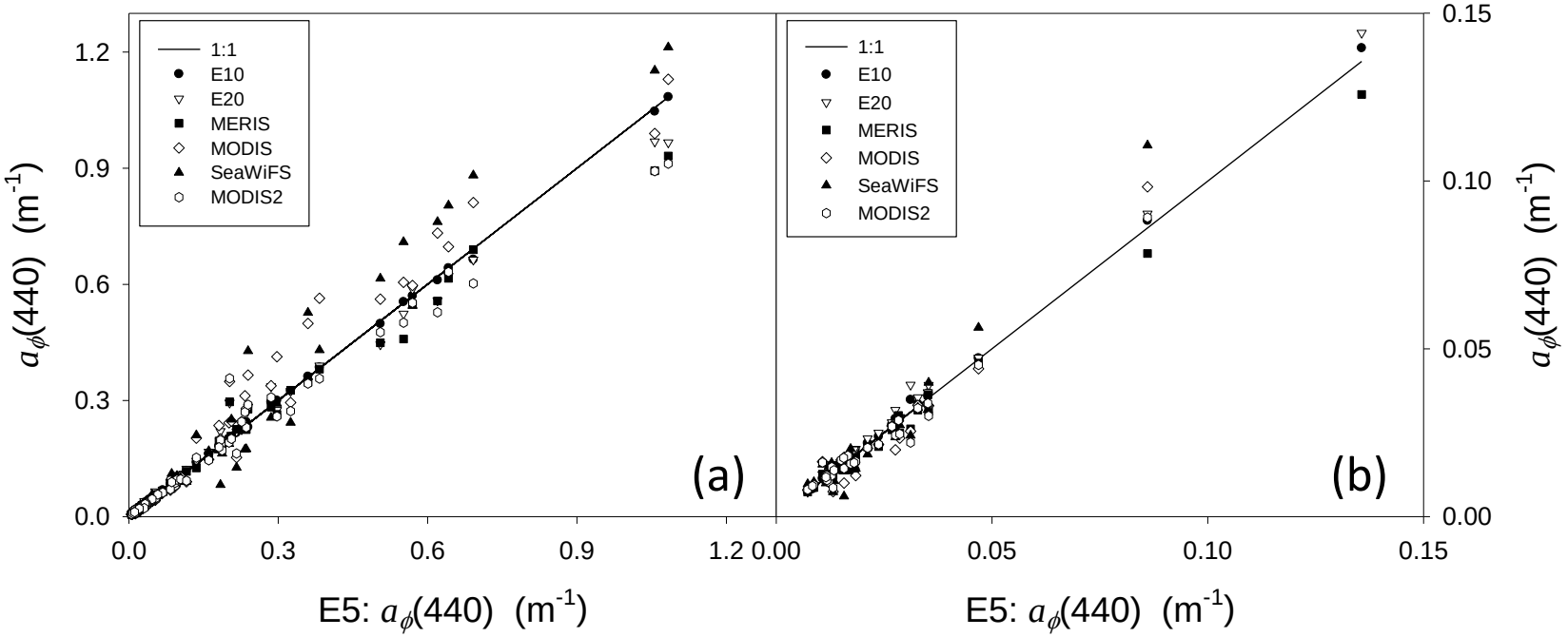

(Lee and Carder 2002)

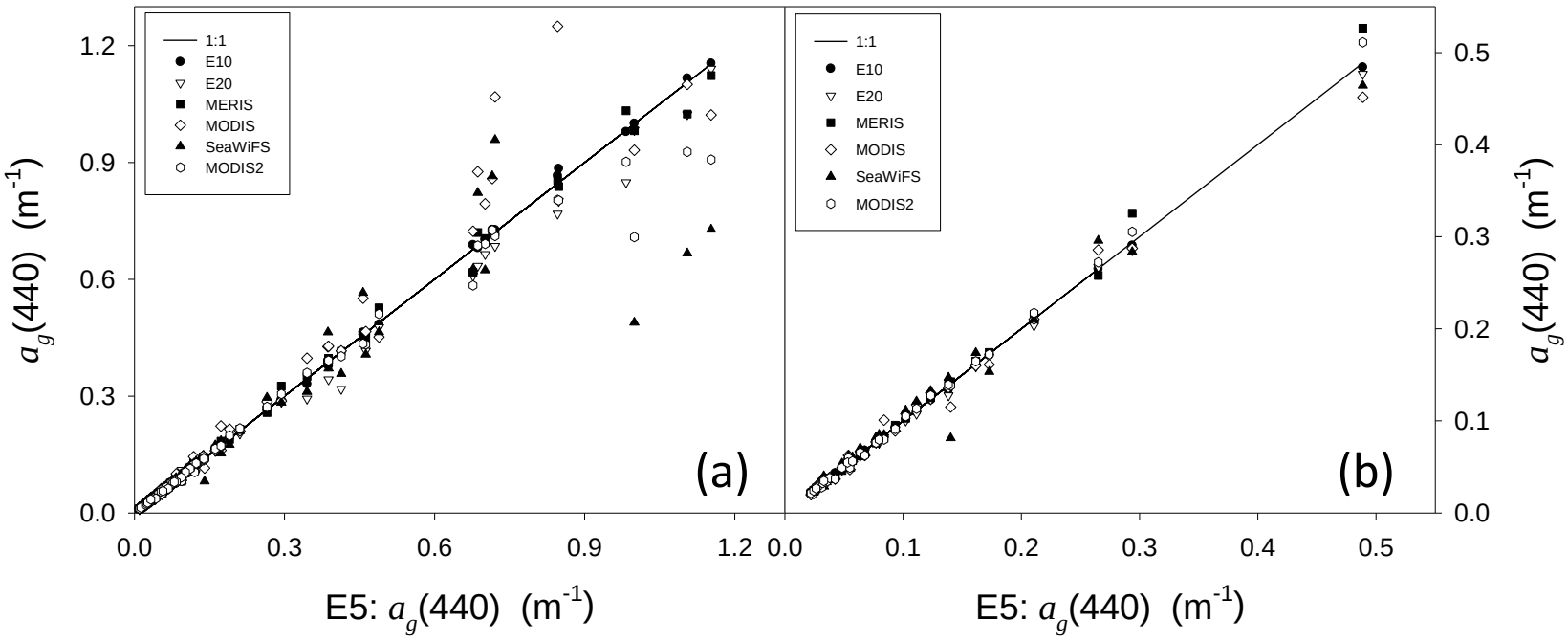
1:1
E10
E20
MERIS
MODIS
SeaWiFS
MODIS2
(a)
(b)
$a_g(440)$ (m^{-1})
E5: $a_g(440)$ (m^{-1})
0.0
0.3
0.6
0.9
1.2
0.1
0.2
0.4
0.5

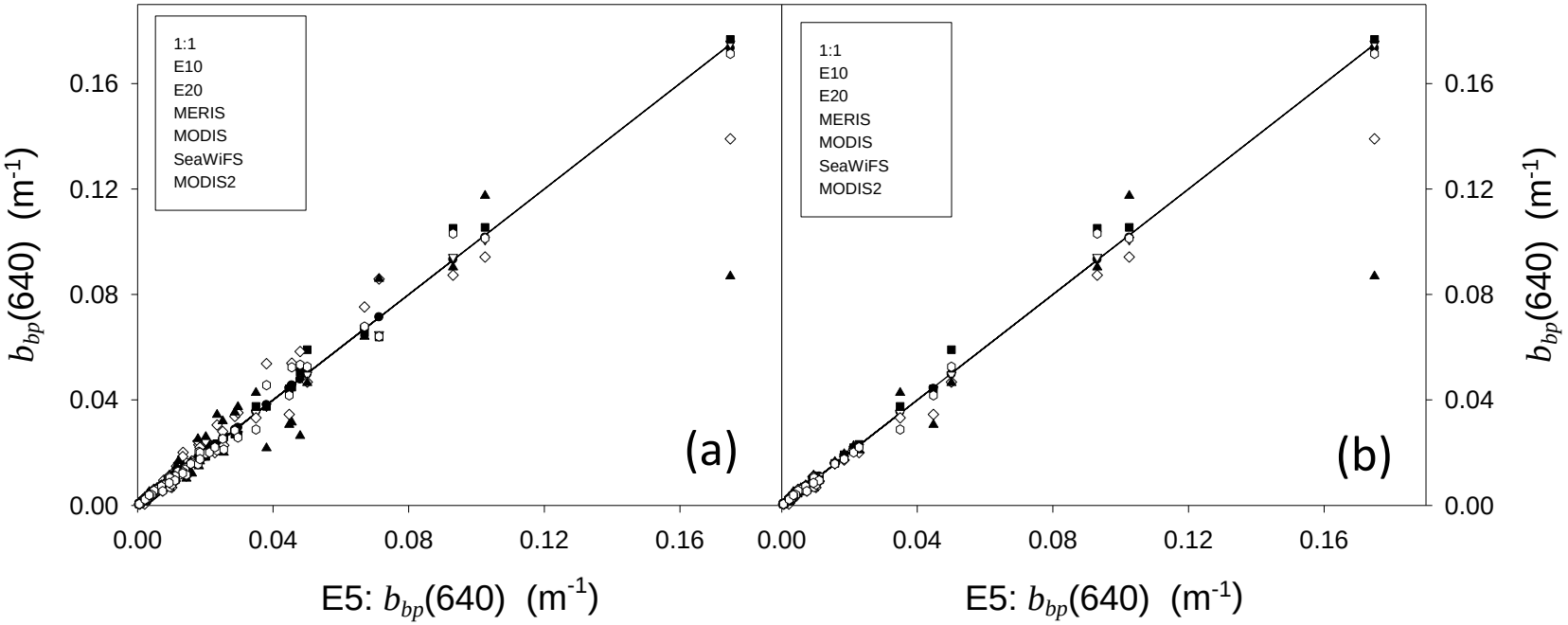
1:1
E10
E20
MERIS
MODIS
SeaWiFS
MODIS2
(a)
(b)
b_{bp}(640) (m^{-1})
E5: b_{bp}(640) (m^{-1})
0.00
0.04
0.08
0.12
0.16

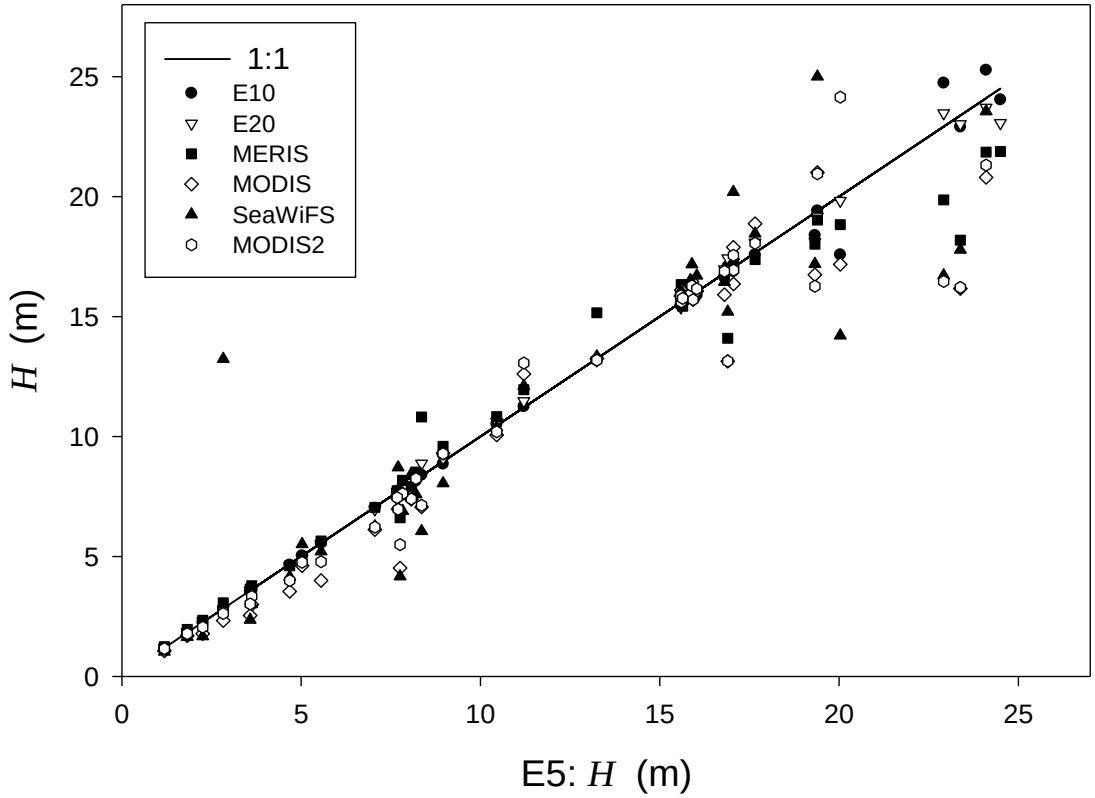

Retrievals with Rrs of ~15 bands are equivalent to that from hyperspectral Rrs.

Why?

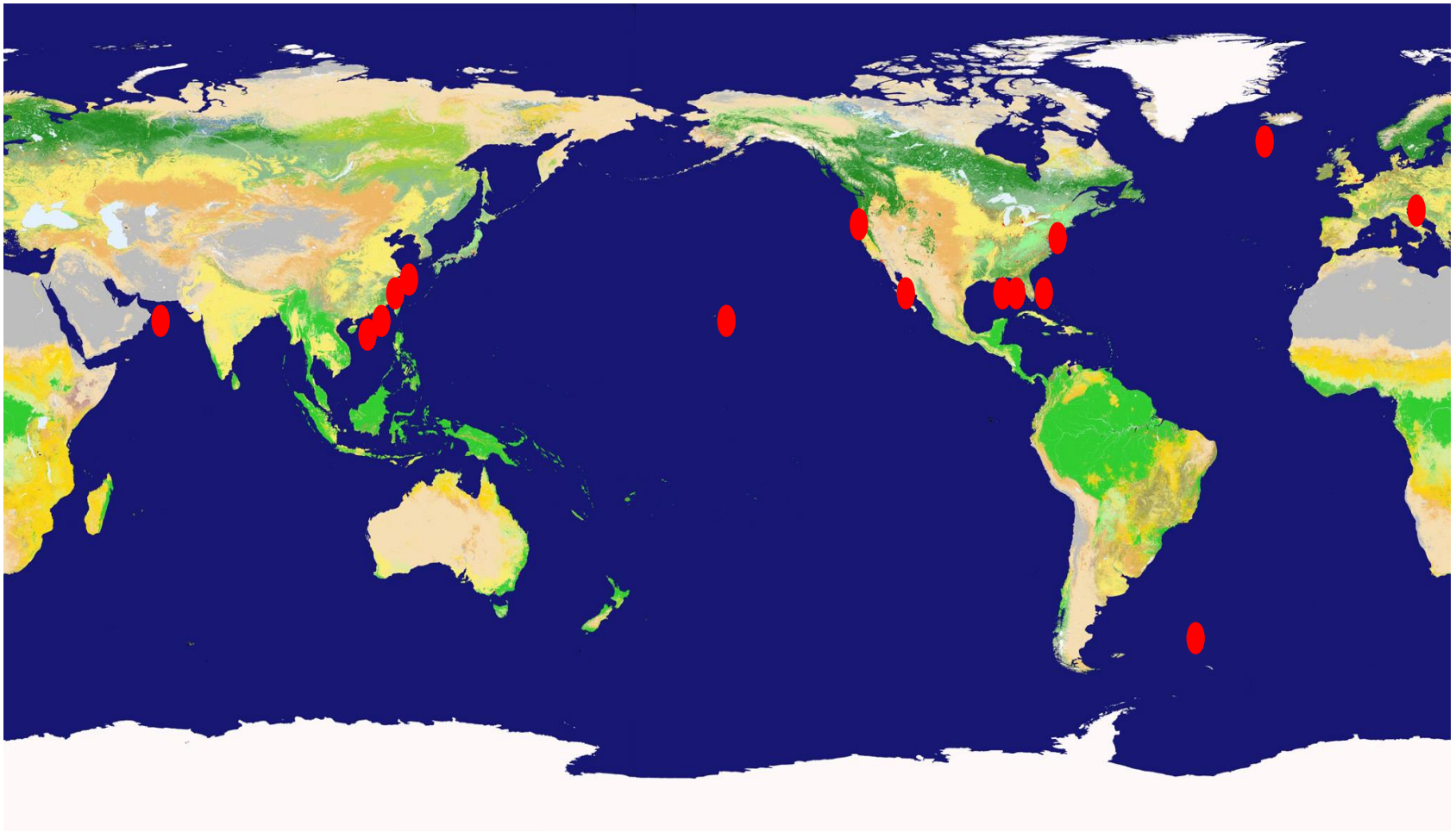

Characteristics of Rrs dataset (~1000 spectra)

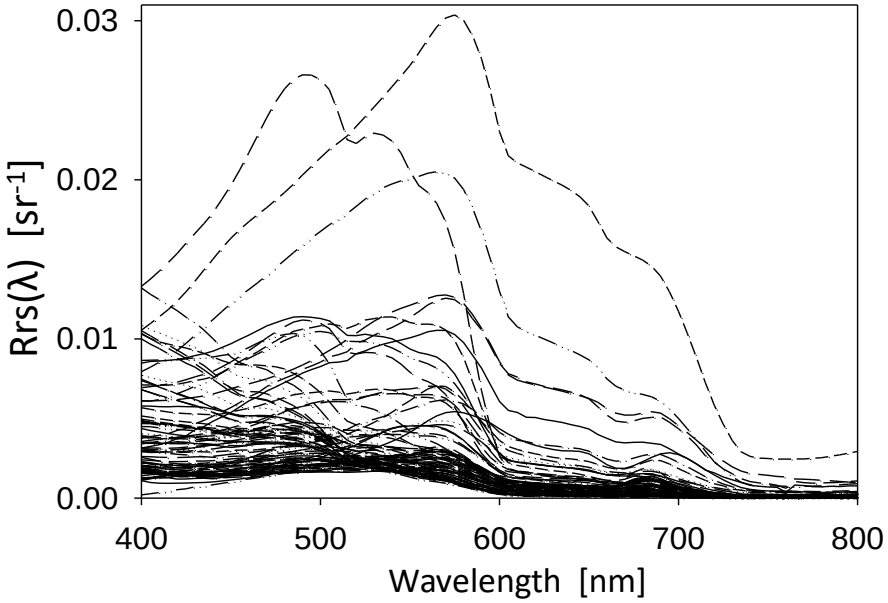

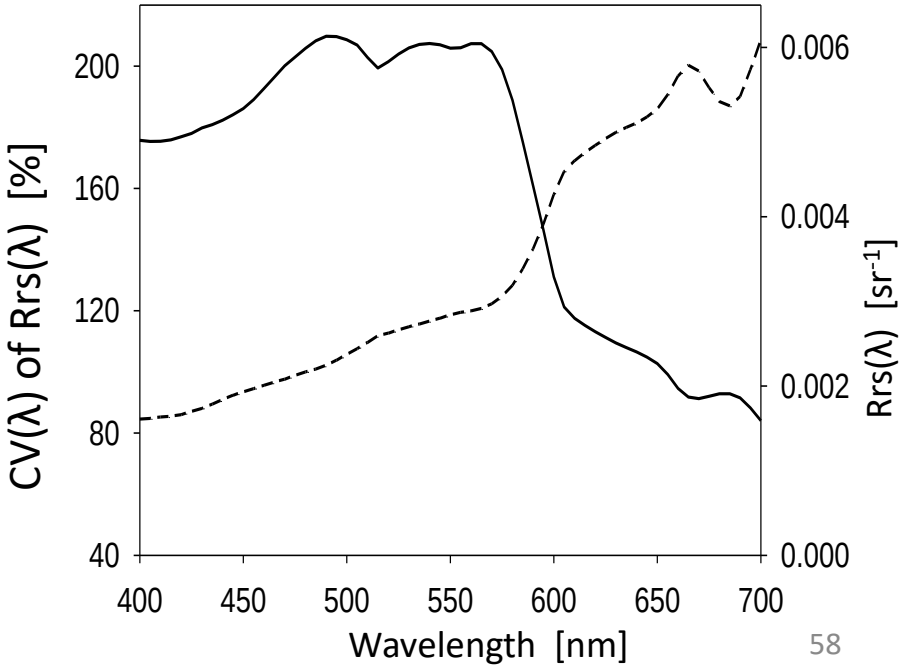

Correlation coefficient of Rrs between neighbor bands:

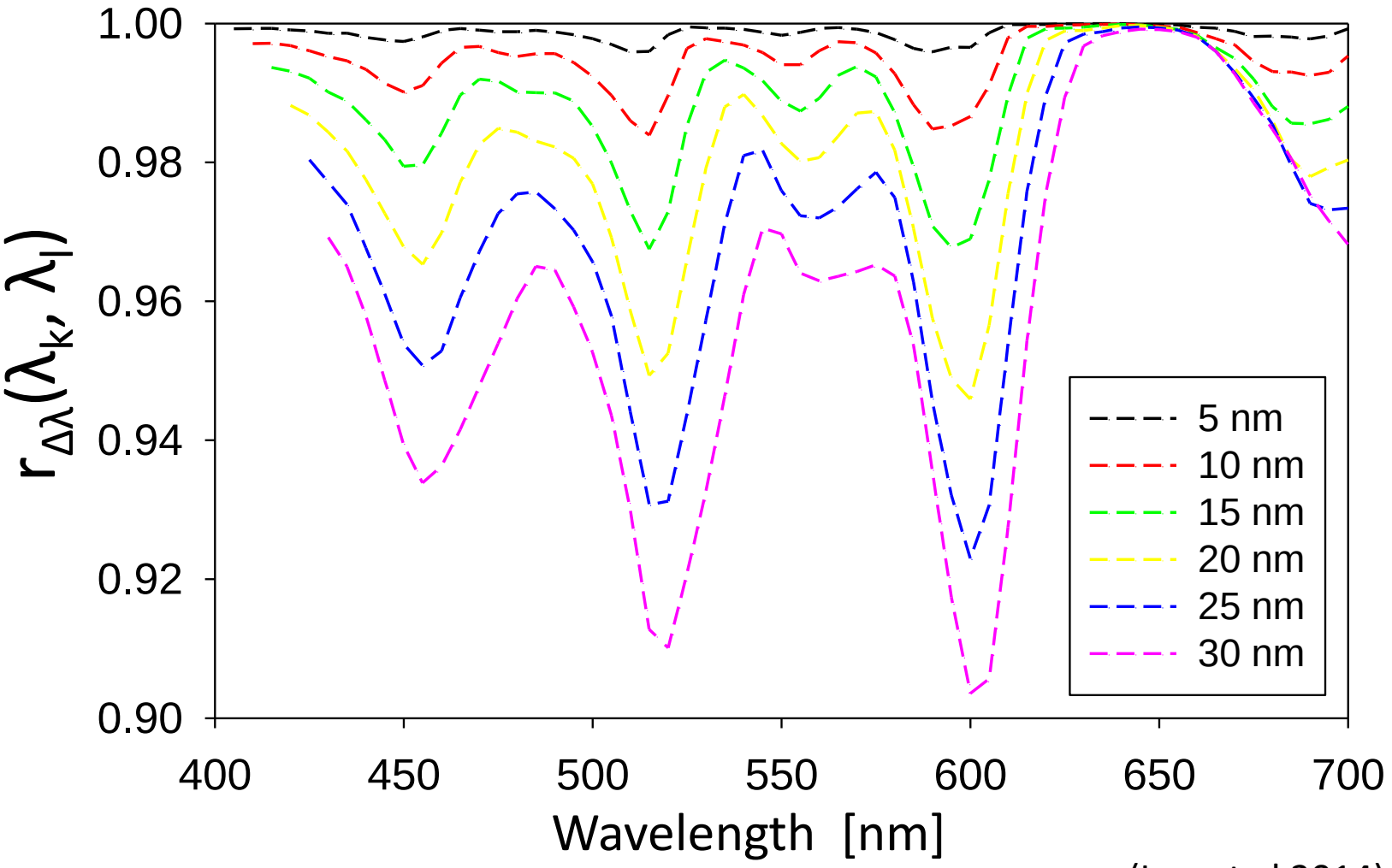

(Lee et al 2014)

Spectral Rrs are highly correlated, especially for short gaps in wavelengths

$$R_{rs}(\lambda) = G \frac{b_{bw}(\lambda) + b_{bp}(\lambda)}{a_w(\lambda) + a_x(\lambda) + b_{bw}(\lambda) + b_{bp}(\lambda)}$$

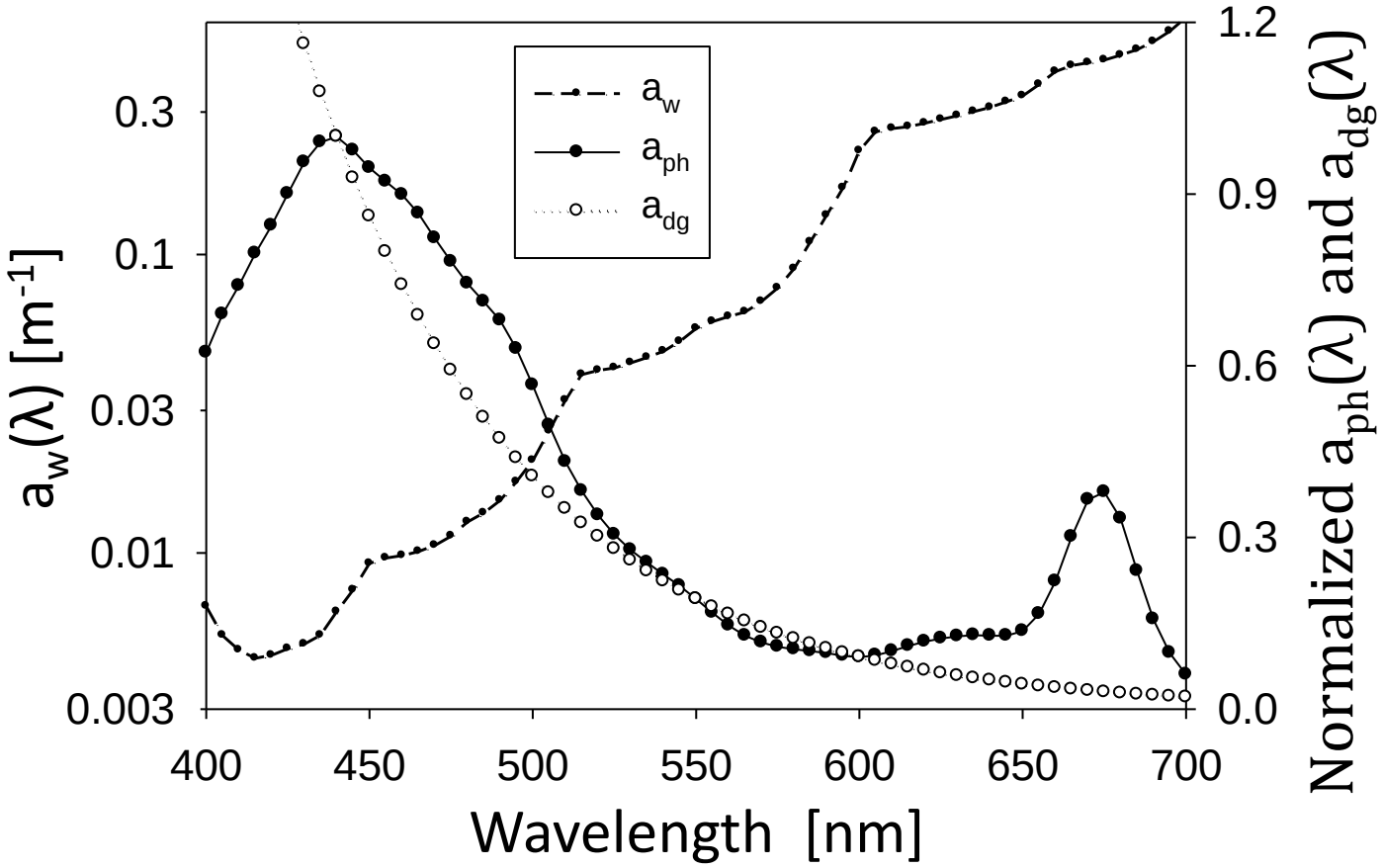

Re-construct hyperspectral Rrs from multi-band Rrs

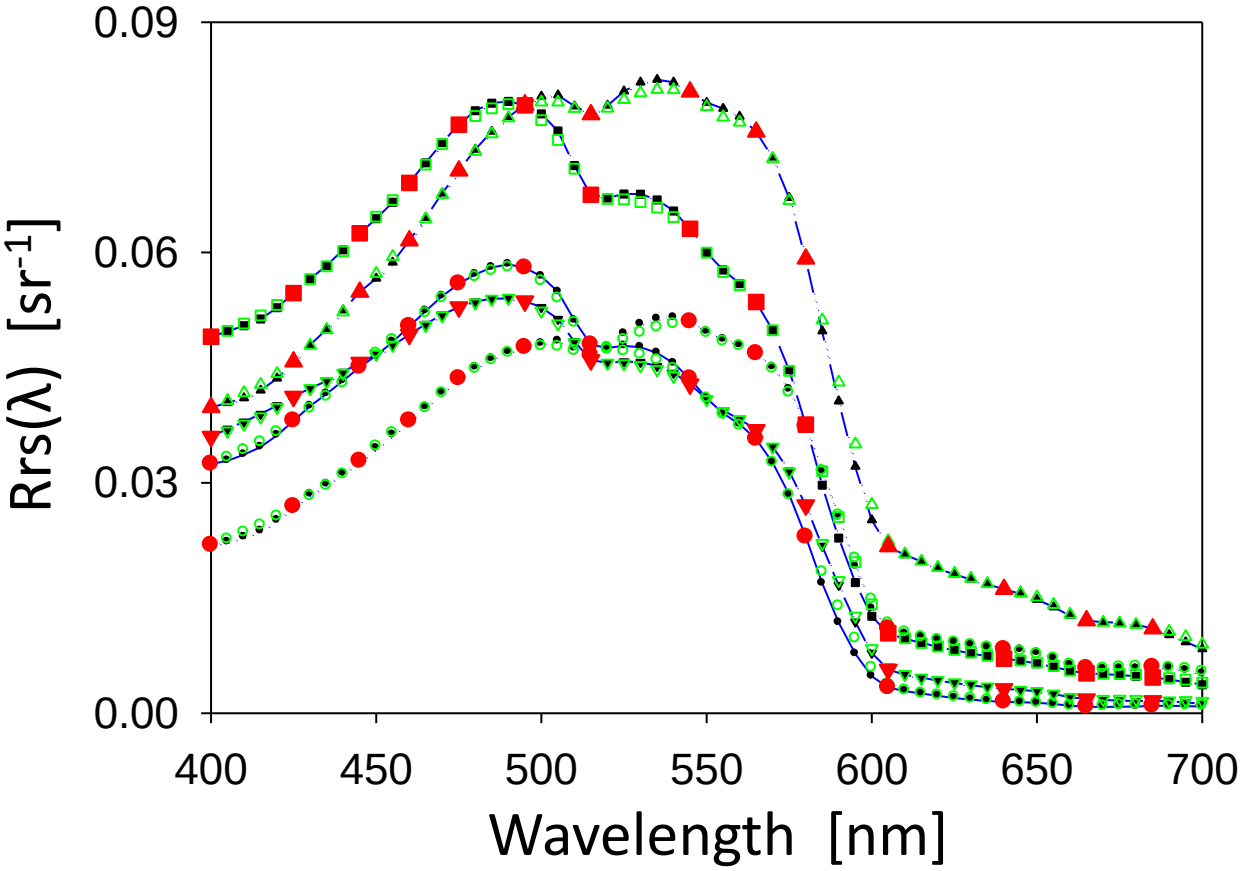

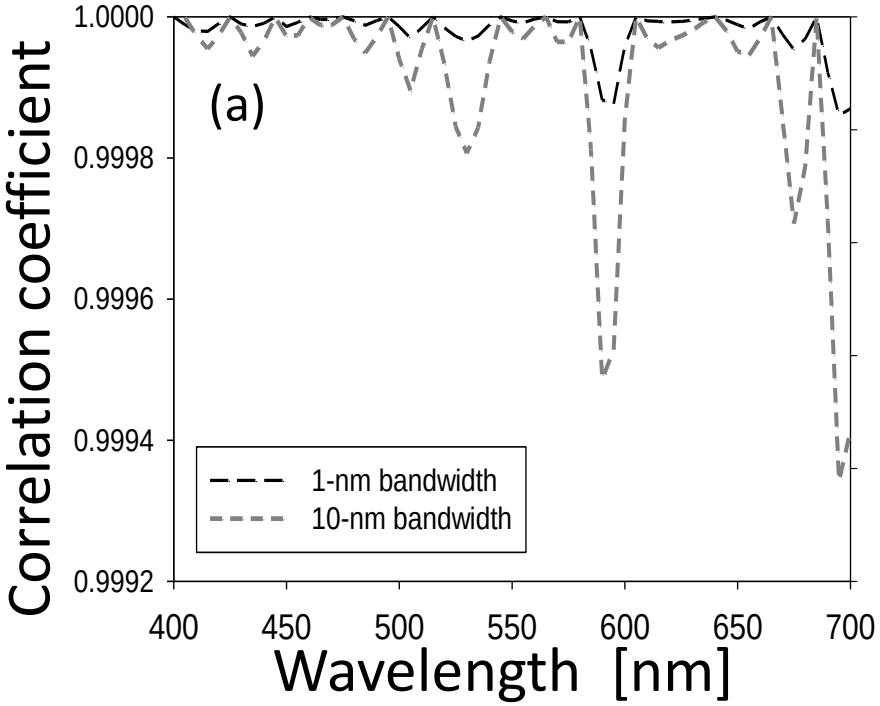

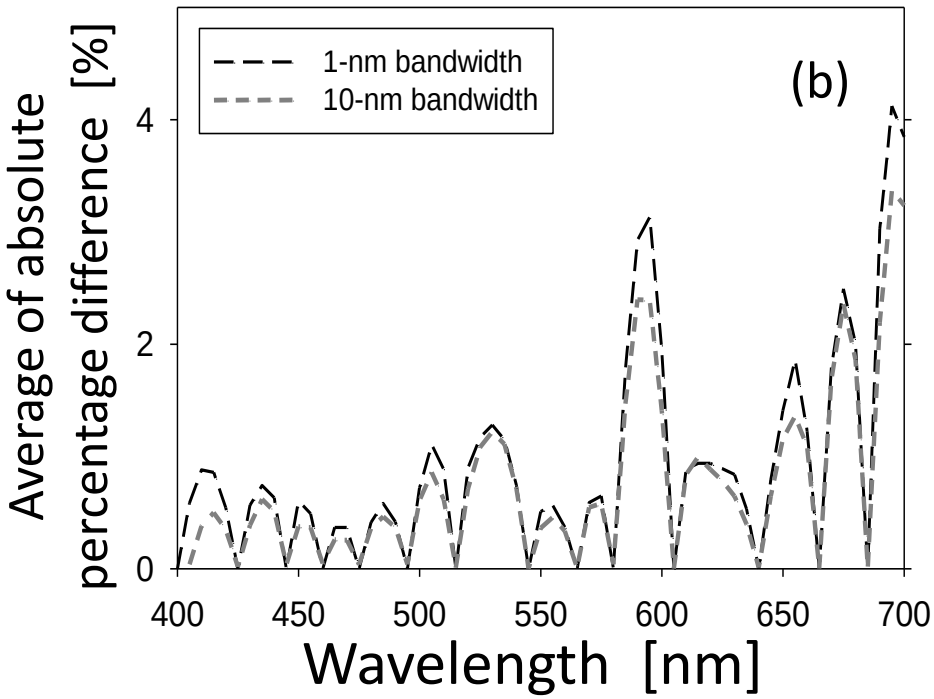

(Lee et al 2014)

hyperspectral Rrs can be well re-constructed from Rrs of ~15 bands

b). Effect of bandwidth

IOPs of wide-spectral bands

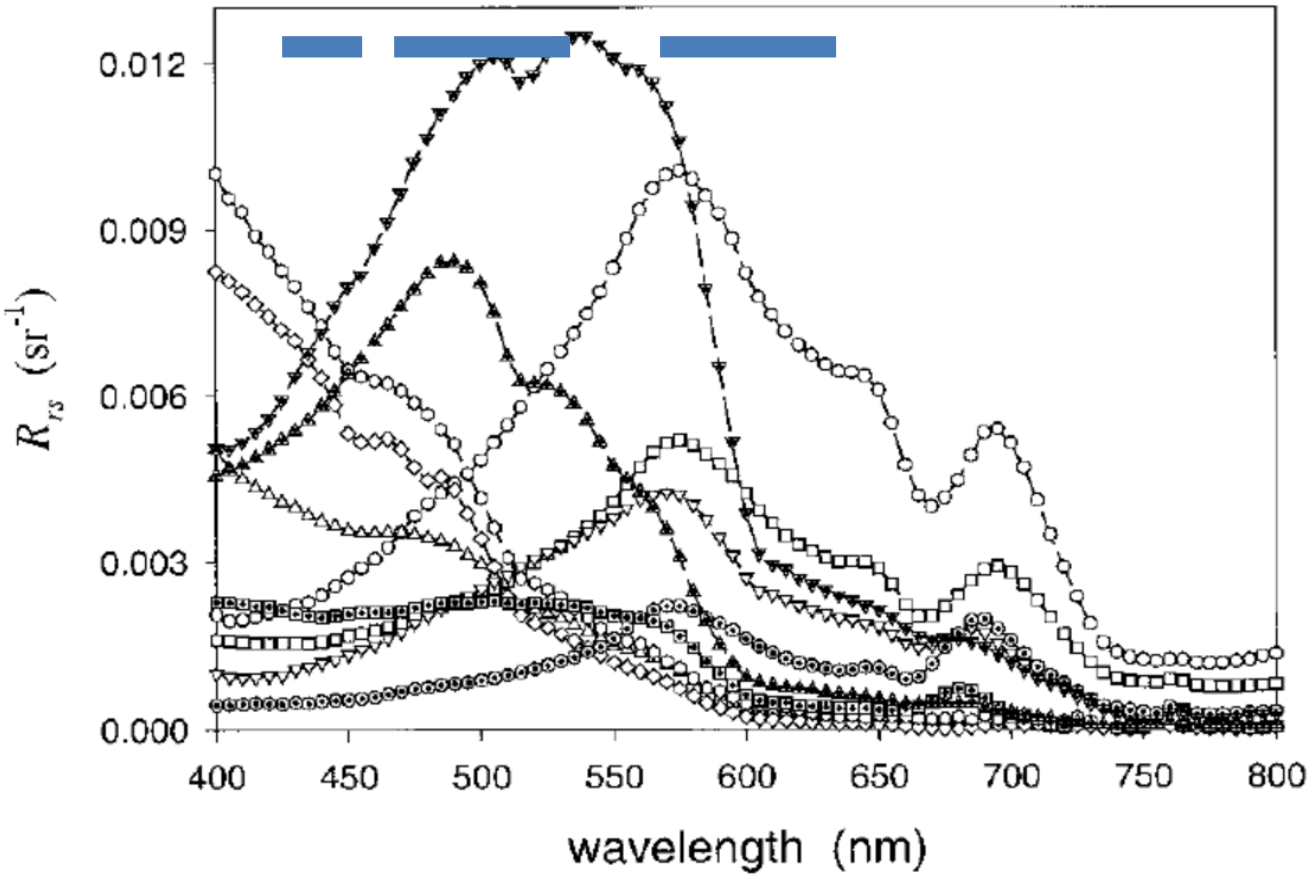

Landsat 8

$$R_{rs}(\lambda) = G\frac{b_{bw}(\lambda)+b_{bp}(\lambda)}{a_w(\lambda)+a_x(\lambda)+b_{bw}(\lambda)+b_{bp}(\lambda)}$$

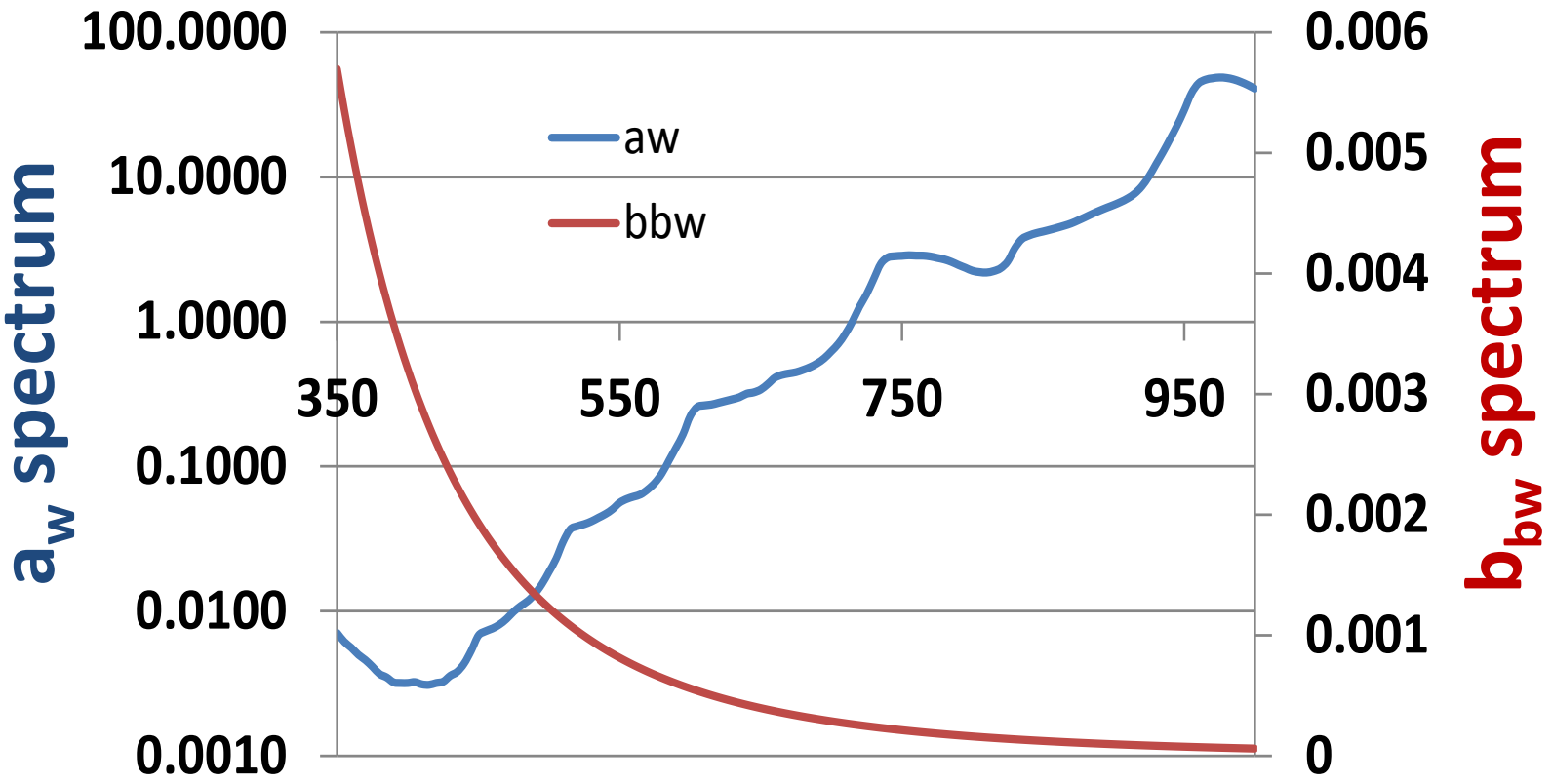

Band-averaged pure-water constants for remote sensing?

“standard” approach:

$$a_w(i) = integral\left\{\frac{a_w(\lambda) * RSRi(\lambda) * d\lambda}{intergral\{RSR_i(\lambda) * d\lambda\}}\right\}$$

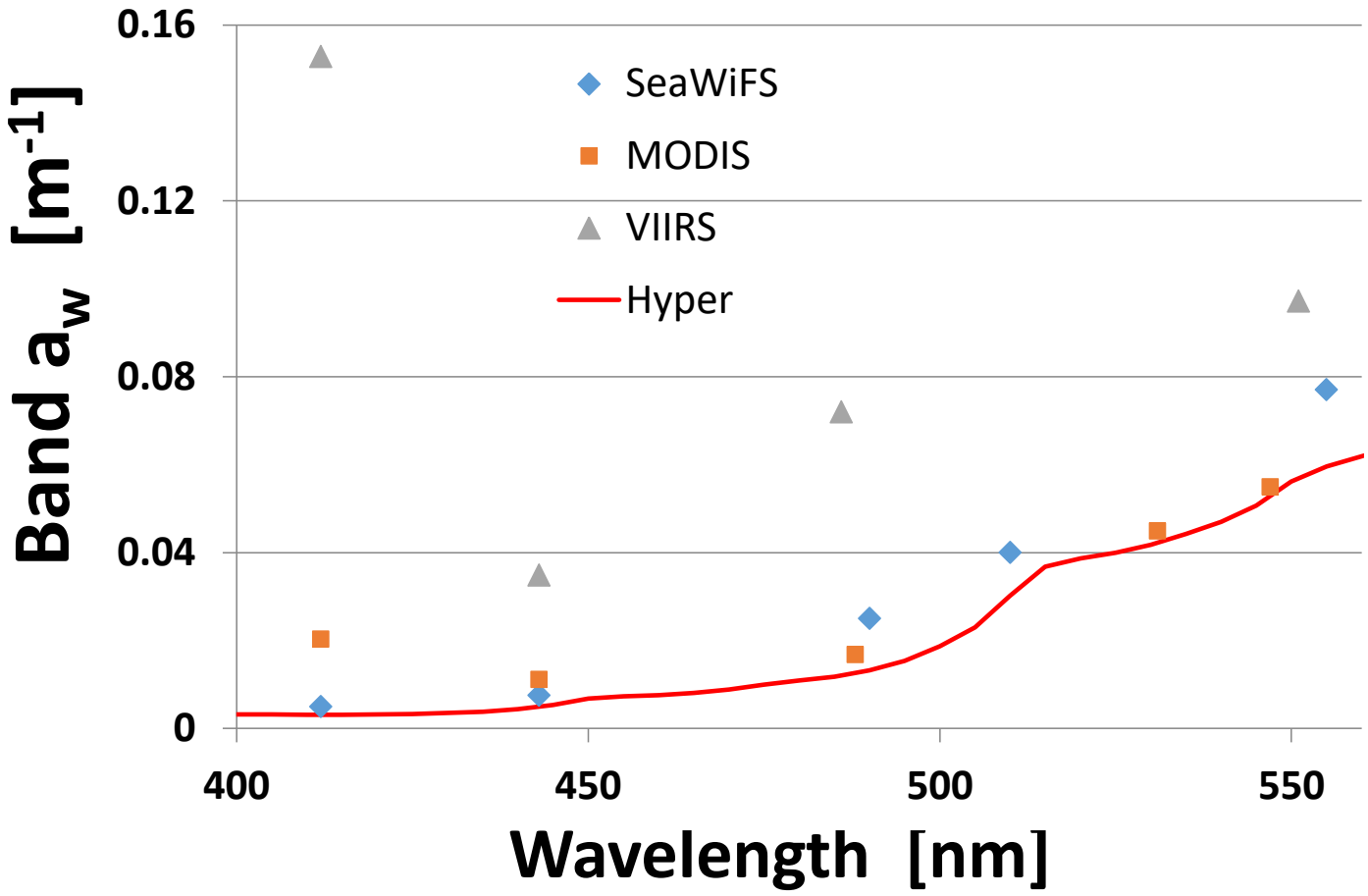

→ Consequence is no closure of Rrs

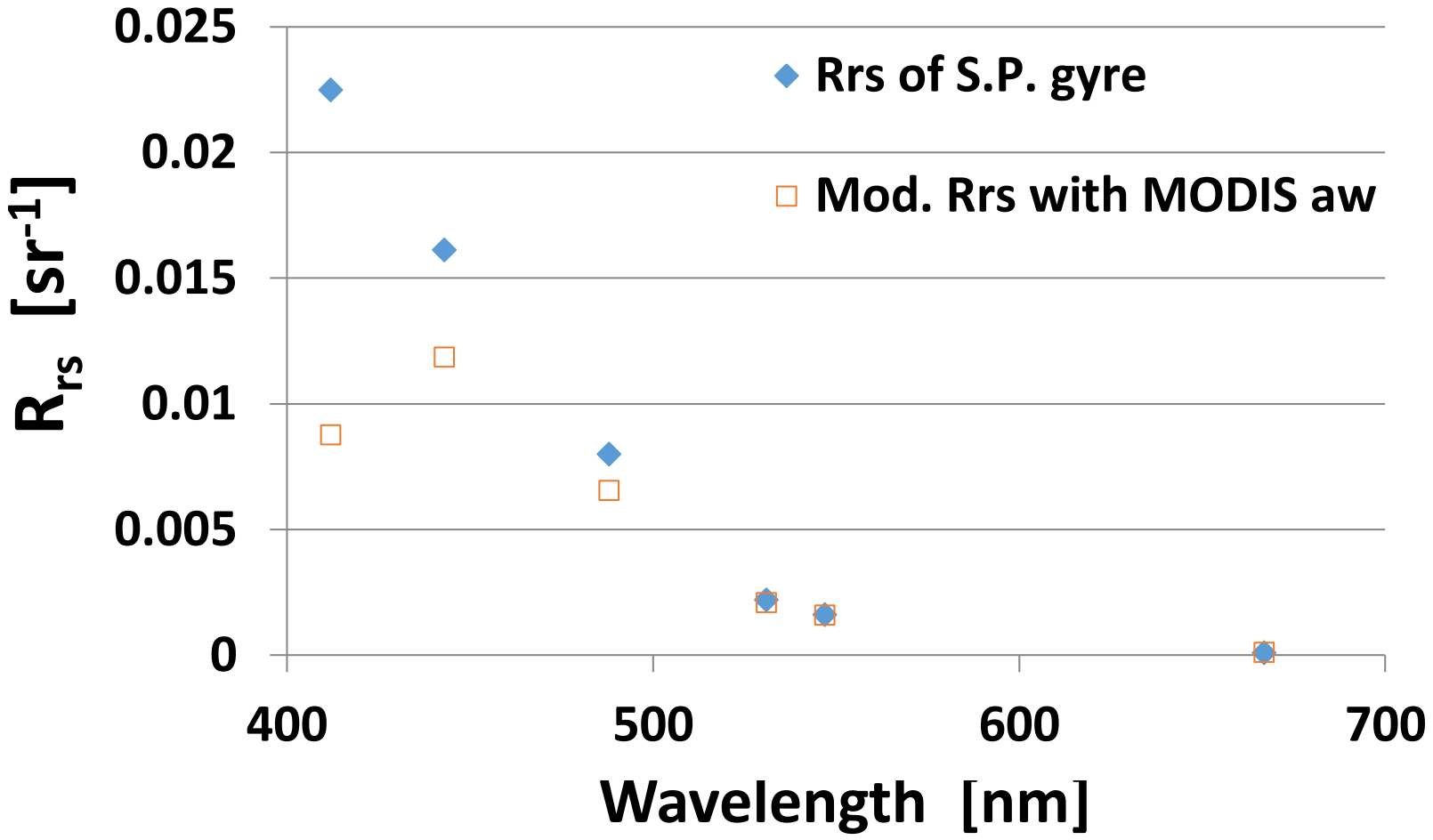

$$R_{rs}(\lambda) = G \frac{b_{bw}(\lambda) + b_{bp}(\lambda)}{a_w(\lambda) + a_x(\lambda) + b_{bw}(\lambda) + b_{bp}(\lambda)}$$

$$x_w(B_i) = \frac{\int RSR_i(\lambda)\left(1/a_w(\lambda)\right)d\lambda}{\int RSR_i(\lambda)d\lambda}$$

$$a_w(B_i) = \frac{1}{x_w(B_i)}$$

(Lee et al 2016)

→ band-averaged a_w for Rrs

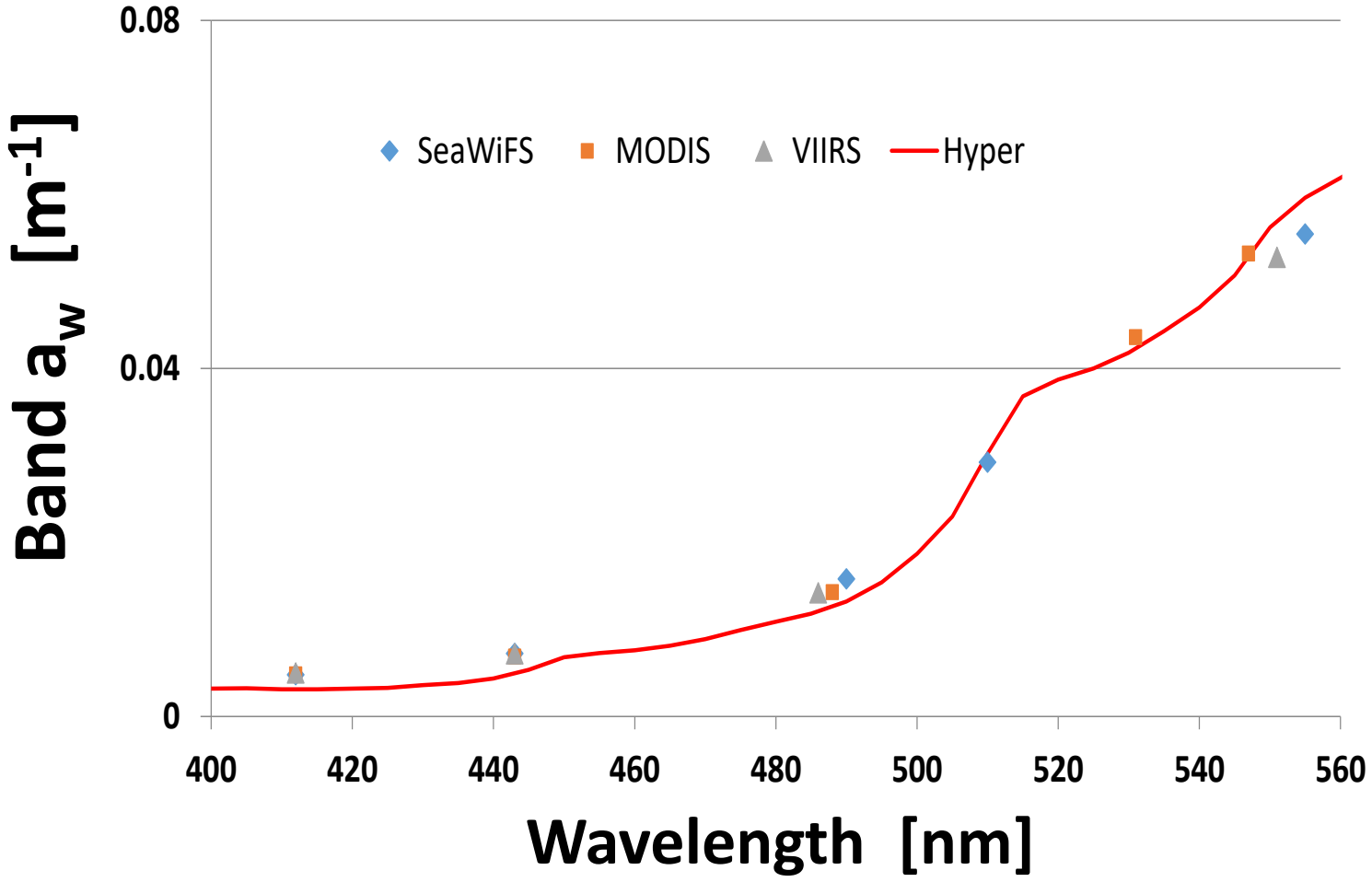

→ Closure of Rrs

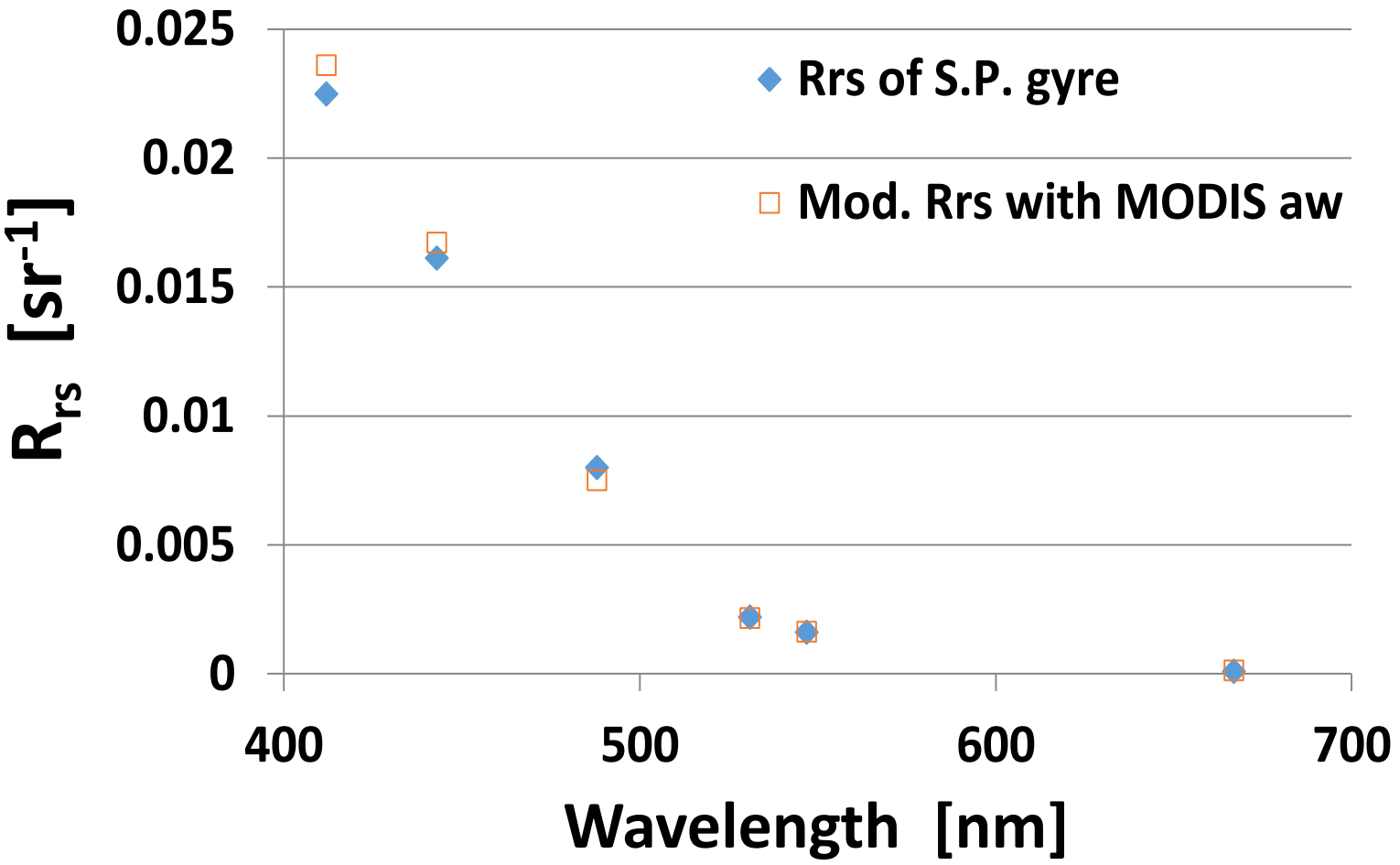

c). Effect of spatial resolution (pixel size)

1 km x 1 km (Low)

30 m x 30 m (High)

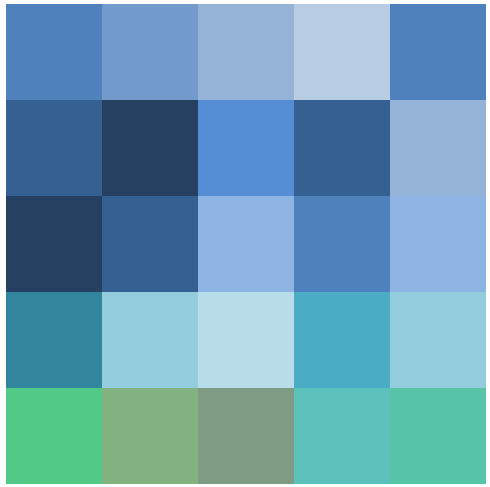

How to compare results from the two observations if the target is not uniform?

$Property_{lo}$ = average of $Property_{hi}$??

Chl_{lo} = average of Chl_{hi} ??

H_{lo} = average of H_{hi} ??

What kind of "average"?

$$R_{rs}(\lambda) = \frac{L_w(\lambda)}{E_d(\lambda)}$$

Arithmetic average

$$Lw_{lo} = \overline{Lw_{hi}(i)}$$

$$Rrs_{lo} = \overline{Rrs_{hi}(i)}$$

$$Rrs = G\frac{b_b}{a + b_b}$$

$$a_{lo} \neq \overline{a_{hi}(i)}$$

Chl_{lo} ≠ average of Chl_{hi}

$$g' \frac{b_b{}^{Lo}}{a^{Lo}} \approx \overline{g' \frac{b_b{}^{Hi}(i)}{a^{Hi}(i)}}$$

$$\frac{b_b{}^{Lo}}{a^{Lo}} \approx \frac{1}{n} \sum_{i=1}^{n} \frac{b_b{}^{Hi}(i)}{a^{Hi}(i)}$$

$$a^{Lo} \approx \frac{n\, b_b{}^{Lo} \prod_{i=1}^{n} a^{Hi}(i)}{\sum_{i=1}^{n} \left(b_b{}^{Hi}(i) \prod_{j=1, j \neq i}^{n-1} a^{Hi}(j) \right)}$$

Backscattering weighted average

$$b_b{}^{Lo} \approx \overline{b_b{}^{Hi}(i)}$$

Lee et al (2012)

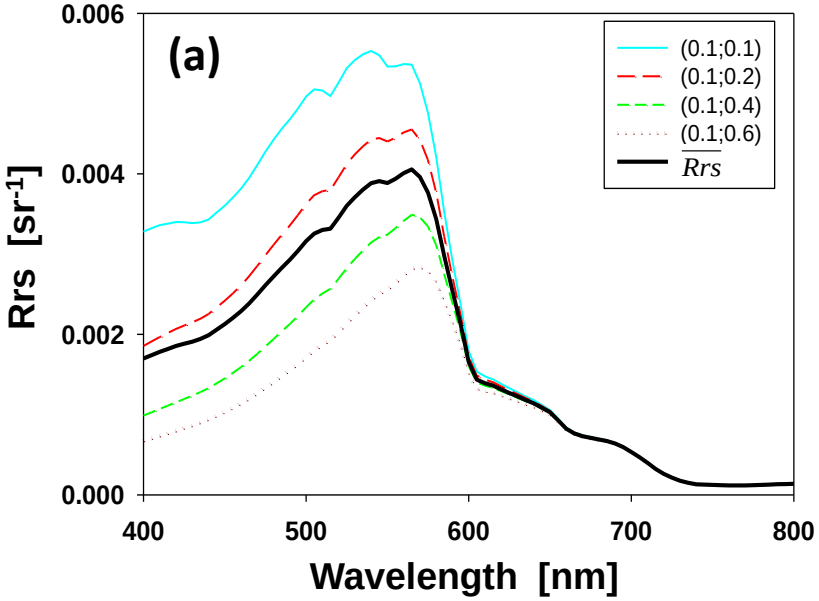
(a)
(0.1;0.1)
(0.1;0.2)
(0.1;0.4)
(0.1;0.6)
$\overline{Rrs}$
Rrs [sr-1]
0.006
0.004
0.002
0.000
400
500
600
700
800
Wavelength [nm]

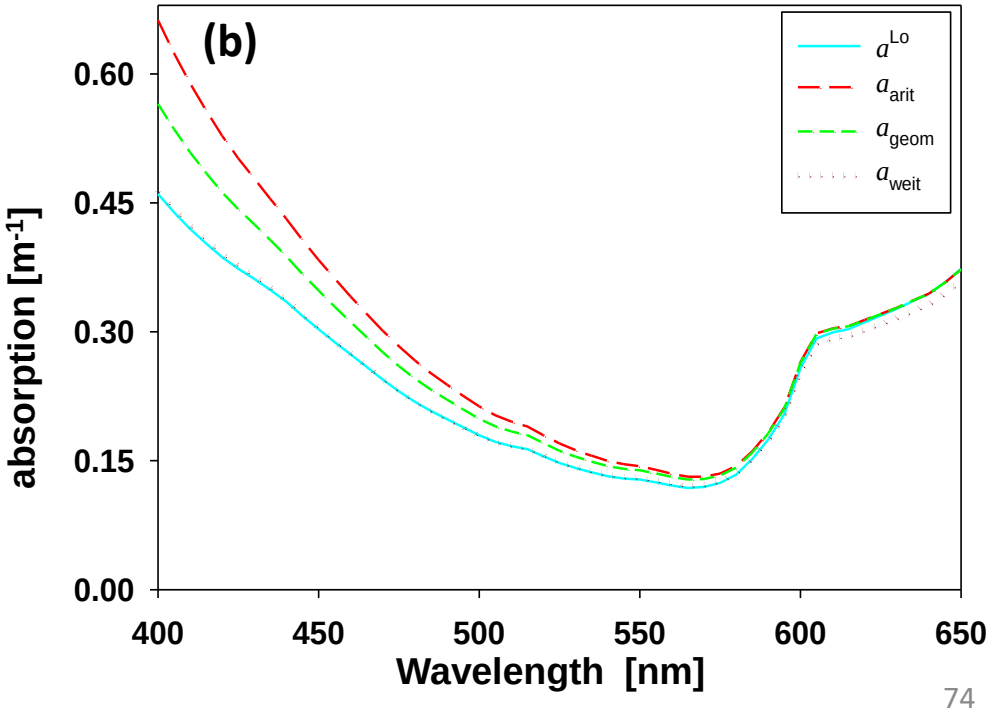
(b)
a^{Lo}
a_{arit}
a_{geom}
a_{weit}
absorption [m-1]
0.60
0.45
0.30
0.15
0.00
400
450
500
550
600
650
Wavelength [nm]

Shallow water:

H_{lo} = average of H_{hi} ??

$$R_{rs} = G(r_{rs}^{C} + r_{rs}^{B}) = G\left[r_{rs}^{dp}\left(1 - e^{-D_c(a+b_b)H}\right) + \frac{\rho}{\pi} e^{-D_B(a+b_b)H}\right]$$

$$\rho^{Lo}\, e^{-D_B(a+b_b)H^{Lo}} \approx \overline{\rho^{Hi}(i)\, e^{-D_B(a+b_b)H^{Hi}(i)}}$$

$$H^{Lo} \approx \frac{-1}{D_B(a+b_b)} \ln\left\{\frac{1}{\rho^{Lo}} \overline{\rho^{Hi}(i)\, e^{-D_B(a+b_b)H^{Hi}(i)}}\right\}$$

Lee et al (2012)

$$\frac{\rho^{Lo}}{H^{Lo}} \approx \overline{\frac{\rho^{Hi}(i)}{H^{Hi}(i)}}$$

$$H^{Lo} \approx \frac{n\,\rho^{Lo}\prod_{i=1}^{n} H^{Hi}(i)}{\sum_{i=1}^{n}\left(\rho^{Hi}(i)\prod_{j=1,\,j\neq i}^{n-1} H^{Hi}(j)\right)}$$

For same type of bottom:

$$H^{Lo} \approx \frac{n}{\sum_{i=1}^{n}\overline{\frac{1}{H^{Hi}(i)}}}$$

Lee et al (2012)

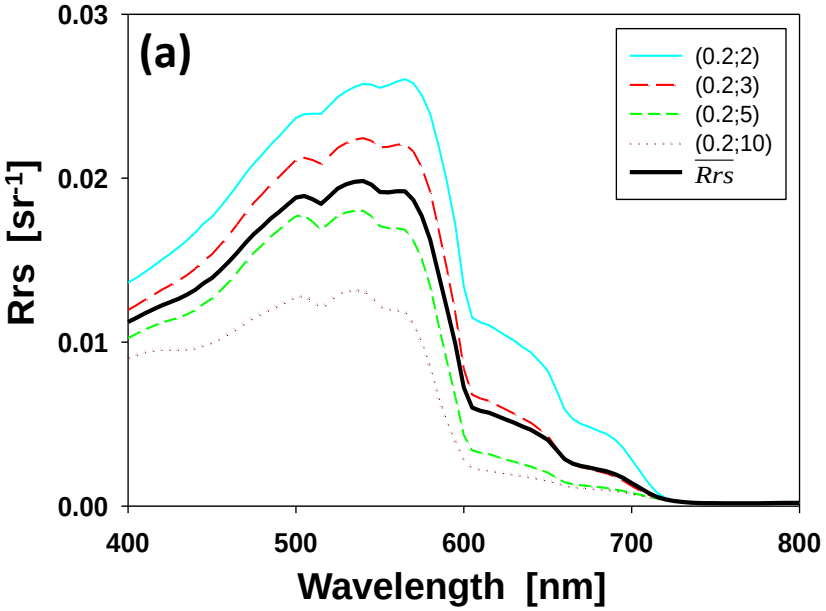

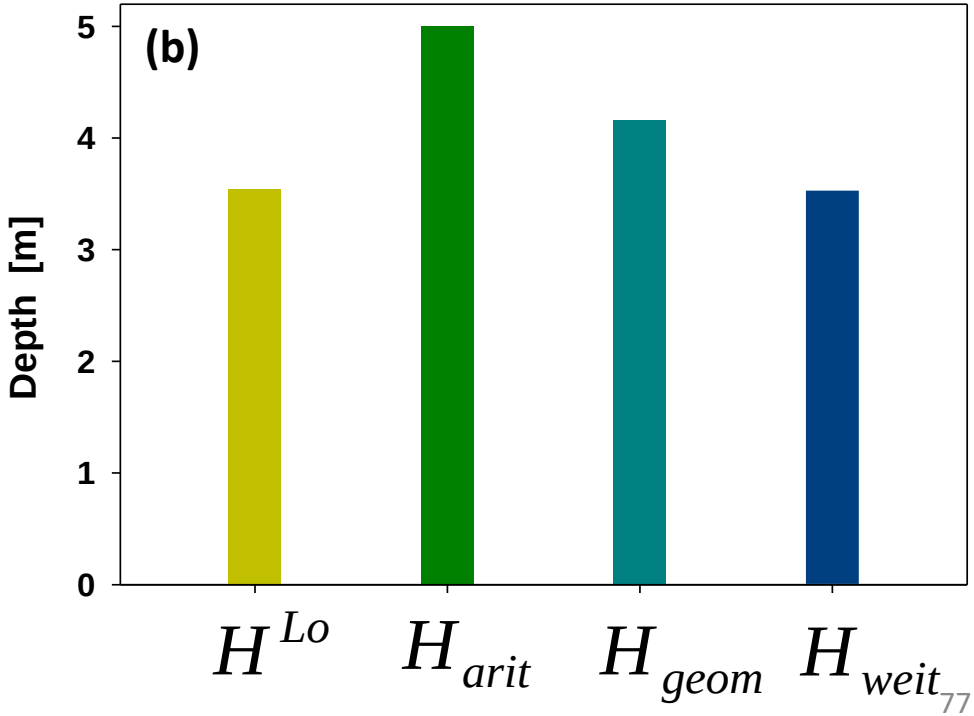

Lee et al (2012)

Key Points:

1. Various inversion algorithms for IOPs have been developed; but more/better ones are also expected.

2. BUS derives every component first, then (simultaneously) derives the total optical property.

Assume the spectral shapes of the optically active components are well characterized.
BUS relies more on the accuracy of forward bio-optical models.

3. TDS derives total first, then decompose it to separate components.

TDS relies more on the accuracy of Rrs measurement

4. Spectral details of input Rrs have various impact on the analytical retrieval of IOPs.

5. For spatially varying water properties, it is necessary to be careful to compare properties of different pixel sizes. It may not be a simply arithmetic average.

References:

Ocean color chlorophyll algorithms for SeaWiFS

John E. O'Reilly,[1] Stéphane Maritorena,[2] B. Greg Mitchell,[3] David A. Siegel,[4] Kendall L. Carder,[5] Sara A. Garver,[6] Mati Kahru,[3] and Charles McClain[7]

JOURNAL OF GEOPHYSICAL RESEARCH, VOL. 103, NO. C11, PAGES 24,937–24,953, OCTOBER 15, 1998

Chlorophyll *a* algorithms for oligotrophic oceans: A novel approach based on three-band reflectance difference

Chuanmin Hu,[1] Zhongping Lee,[2] and Bryan Franz[3]

JOURNAL OF GEOPHYSICAL RESEARCH, VOL. 117, C01011, doi:10.1029/2011JC007395, 2012

An empirical algorithm for light absorption by ocean water based on color

Z. P. Lee, K. L. Carder, R. G. Steward, and T. G. Peacock

Department of Marine Science, University of South Florida, St. Petersburg

JOURNAL OF GEOPHYSICAL RESEARCH, VOL. 103, NO. C12, PAGES 27,967–27,978, NOVEMBER 15, 1998

Absorption Coefficient and Chlorophyll Concentration of Oceanic Waters Estimated from Band Difference of Satellite-Measured Remote Sensing Reflectance

Zhongping Lee[1*], Longteng Zhao[1], Chuanmin Hu[2], Daosheng Wang[1], Junfang Lin[3], and Shaoling Shang[1]

Journal of Remote Sensing
A SCIENCE PARTNER JOURNAL

Lee et al. 2023 | https://doi.org/10.34133/remotesensing.0063

A theoretical derivation of the dependence of the remotely sensed reflectance of the ocean on the inherent optical properties

J. Ronald V. Zaneveld

JOURNAL OF GEOPHYSICAL RESEARCH, VOL. 100, NO. C7, PAGES 13,135–13,142, JULY 15, 1995

Article

Ocean Color Analytical Model Explicitly Dependent on the Volume Scattering Function

Michael Twardowski [1,2,*] and Alberto Tonizzo [2,*]

Appl. Sci. **2018**, *8*, 2684; doi:10.3390/app8122684

An analytical model for subsurface irradiance and remote sensing reflectance in deep and shallow case-2 waters

A. Albert
German Aerospace Center (DLR), Remote Sensing Technology Institute, D-82230 Wessling, Germany
andreas.albert@dlr.de

C.D. Mobley
Sequoia Scientific Inc., 2700 Richards Road, Suite 107, Bellevue, WA 98005 USA
mobley@sequoiasci.com

3 November 2003 / Vol. 11, No. 22 / OPTICS EXPRESS 2873

Model of remote-sensing reflectance including bidirectional effects for case 1 and case 2 waters

Young-Je Park and Kevin Ruddick

1236 APPLIED OPTICS / Vol. 44, No. 7 / 1 March 2005

HYDROPT: A fast and flexible method to retrieve chlorophyll-a from multispectral satellite observations of optically complex coastal waters

Hendrik Jan Van Der Woerd *, Reinold Pasterkamp

Remote Sensing of Environment 112 (2008) 1795 – 1807

Diffuse reflectance of oceanic waters. II. Bidirectional aspects

André Morel and Bernard Gentili

6864 APPLIED OPTICS / Vol. 32, No. 33 / 20 November 1993

Diffuse reflectance of oceanic waters. III. Implication of bidirectionality for the remote-sensing problem

André Morel and Bernard Gentili 4850 APPLIED OPTICS / Vol. 35, No. 24 / 20 August 1996

A Semianalytic Radiance Model of Ocean Color

HOWARD R. GORDON,[1] OTIS B. BROWN,[2] ROBERT H. EVANS,[2] JAMES W. BROWN,[1]
RAYMOND C. SMITH,[3] KAREN S. BAKER,[4] AND DENNIS K. CLARK[5]

JOURNAL OF GEOPHYSICAL RESEARCH, VOL. 93, NO. D9, PAGES 10,909–10,924, SEPTEMBER 20, 1988

Effects of molecular and particle scatterings on the model parameter for remote-sensing reflectance

ZhongPing Lee, Kendall L. Carder, and KePing Du

1 September 2004 / Vol. 43, No. 25 / APPLIED OPTICS 4957

Variability in the chlorophyll-specific absorption coefficients of natural phytoplankton: Analysis and parameterization

Annick Bricaud, Marcel Babin, André Morel, and Hervé Claustre

JOURNAL OF GEOPHYSICAL RESEARCH, VOL. 100, NO. C7, PAGES 13,321–13,332, JULY 15, 1995

Hyperspectral remote sensing for shallow waters. I. A semianalytical model

Zhongping Lee, Kendall L. Carder, Curtis D. Mobley, Robert G. Steward, and Jennifer S. Patch

20 September 1998 / Vol. 37, No. 27 / APPLIED OPTICS 6329

Assessment of the relationships between dominant cell size in natural phytoplankton communities and the spectral shape of the absorption coefficient

Áurea M. Ciotti,[1] Marlon R. Lewis, and John J. Cullen[2]

Limnol. Oceanogr., 47(2), 2002, 404–417

Determination of the Major Groups of Phytoplankton Pigments From the Absorption Spectra of Total Particulate Matter

NICOLAS HOEPFFNER[1] AND SHUBHA SATHYENDRANATH[2]

JOURNAL OF GEOPHYSICAL RESEARCH, VOL. 98, NO. C12, PAGES 22,789–22,803, DECEMBER 15, 1993

Absorption by dissolved organic matter of the sea (yellow substance) in the UV and visible domains[1]

Annick Bricaud, André Morel, and Louis Prieur *Limnol. Oceanogr.*, 26(1), 1981, 43–53

A three-component model of ocean colour and its application to remote sensing of phytoplankton pigments in coastal waters

S. SATHYENDRANATH†, L. PRIEUR and A. MOREL

INT. J. REMOTE SENSING, 1989, VOL. 10, NO. 8, 1373–1394

Satellite retrieval of inherent optical properties by linear matrix inversion of oceanic radiance models: An analysis of model and radiance measurement errors

Frank E. Hoge
NASA Goddard Space Flight Center, Wallops Flight Facility, Wallops Island, Virginia

Paul E. Lyon

JOURNAL OF GEOPHYSICAL RESEARCH, VOL. 101, NO. C7, PAGES 16,631–16,648, JULY 15, 1996

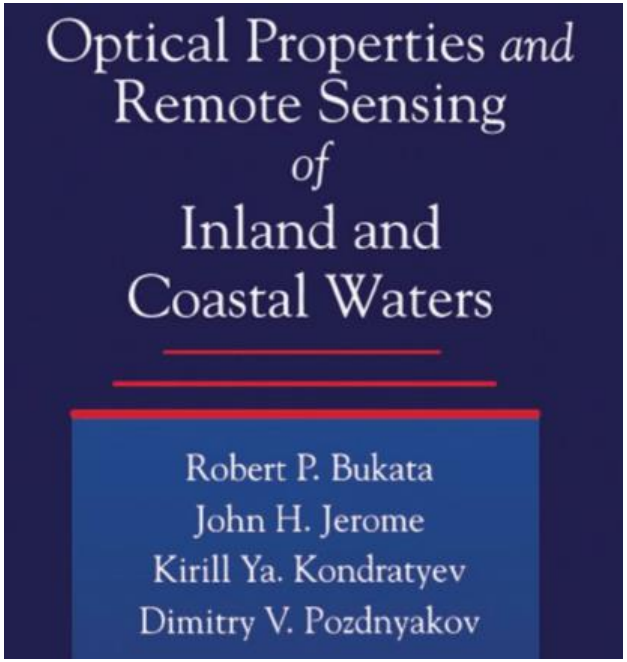

1994

Semianalytic Moderate-Resolution Imaging Spectrometer algorithms for chlorophyll *a* and absorption with bio-optical domains based on nitrate-depletion temperatures

K. L. Carder, F. R. Chen, Z. P. Lee, and S. K. Hawes

JOURNAL OF GEOPHYSICAL RESEARCH, VOL. 104, NO. C3, PAGES 5403–5421, MARCH 15, 1999

Optimization of a semianalytical ocean color model for global-scale applications

Stéphane Maritorena, David A. Siegel, and Alan R. Peterson

20 May 2002 / Vol. 41, No. 15 / APPLIED OPTICS 2705

Generalized ocean color inversion model for retrieving marine inherent optical properties

P. Jeremy Werdell,[1,2,*] Bryan A. Franz,[1] Sean W. Bailey,[1,3] Gene C. Feldman,[1] Emmanuel Boss,[2] Vittorio E. Brando,[4] Mark Dowell,[5] Takafumi Hirata,[6] Samantha J. Lavender,[7] ZhongPing Lee,[8] Hubert Loisel,[9] Stéphane Maritorena,[10] Fréderic Mélin,[5] Timothy S. Moore,[11] Timothy J. Smyth,[12] David Antoine,[13] Emmanuel Devred,[14] Odile Hembise Fanton d'Andon,[15] and Antoine Mangin[15]

1 April 2013 / Vol. 52, No. 10 / APPLIED OPTICS 2019

Interpretation of hyperspectral remote-sensing imagery by spectrum matching and look-up tables

Curtis D. Mobley, Lydia K. Sundman, Curtiss O. Davis, Jeffrey H. Bowles, Trijntje Valerie Downes, Robert A. Leathers, Marcos J. Montes, William Paul Bissett, David D. R. Kohler, Ruth Pamela Reid, Eric M. Louchard, and Arthur Gleason

3576 APPLIED OPTICS / Vol. 44, No. 17 / 10 June 2005

Remote chlorophyll-*a* retrieval in turbid, productive estuaries: Chesapeake Bay case study

Anatoly A. Gitelson [a,*], John F. Schalles [b], Christine M. Hladik [c,1]

Remote Sensing of Environment 109 (2007) 464–472

Estimation of the inherent optical properties of natural waters from the irradiance attenuation coefficient and reflectance in the presence of Raman scattering

Hubert Loisel and Dariusz Stramski

20 June 2000 / Vol. 39, No. 18 / APPLIED OPTICS 3001

Deriving inherent optical properties from water color: a multiband quasi-analytical algorithm for optically deep waters

ZhongPing Lee, Kendall L. Carder, and Robert A. Arnone

20 September 2002 / Vol. 41, No. 27 / APPLIED OPTICS 5755

Semianalytical model for the derivation of ocean color inherent optical properties: description, implementation, and performance assessment

Timothy J. Smyth, Gerald F. Moore, Takafumi Hirata, and James Aiken

8116 APPLIED OPTICS / Vol. 45, No. 31 / 1 November 2006

Estimation of light penetration, and horizontal and vertical visibility in oceanic and coastal waters from surface reflectance

Maéva Doron,[1,2,3] Marcel Babin,[2,3] Antoine Mangin,[1] and Odile Hembise[1]

JOURNAL OF GEOPHYSICAL RESEARCH, VOL. 112, C06003, doi:10.1029/2006JC004007, 2007

Uncertainties of inherent optical properties obtained from semianalytical inversions of ocean color

Peng Wang, Emmanuel S. Boss, and Collin Roesler

4074 APPLIED OPTICS / Vol. 44, No. 19 / 1 July 2005

A model for partitioning the light absorption coefficient of natural waters into phytoplankton, nonalgal particulate, and colored dissolved organic components: A case study for the Chesapeake Bay

Guangming Zheng[1,2,3], Dariusz Stramski[4], and Paul M. DiGiacomo[1]

10.1002/2014JC010604

Influence of Raman scattering on ocean color inversion models

Toby K. Westberry,[1,*] Emmanuel Boss,[2] and Zhongping Lee[3]

5552 APPLIED OPTICS / Vol. 52, No. 22 / 1 August 2013

Penetration of UV-visible solar radiation in the global oceans: Insights from ocean color remote sensing

Zhongping Lee,[1] Chuanmin Hu,[2] Shaoling Shang,[3] Keping Du,[4] Marlon Lewis,[5] Robert Arnone,[6] and Robert Brewin[7]

JOURNAL OF GEOPHYSICAL RESEARCH: OCEANS, VOL. 118, 4241–4255, doi:10.1002/jgrc.20308, 2013

On the non-closure of particle backscattering coefficient in oligotrophic oceans

ZhongPing Lee[*,1], Yannick Huot [2]

17 November 2014 | Vol. 22, No. 23 | DOI:10.1364/OE.22.029223 | OPTICS EXPRESS 29223

Effect of spectral band numbers on the retrieval of water column and bottom properties from ocean color data

Zhongping Lee and Kendall L. Carder

20 April 2002 / Vol. 41, No. 12 / APPLIED OPTICS 2191

Spectral interdependence of remote-sensing reflectance and its implications on the design of ocean color satellite sensors

Zhongping Lee,[1,*] Shaoling Shang,[2] Chuanmin Hu,[3] and Giuseppe Zibordi[4]

20 May 2014 / Vol. 53, No. 15 / APPLIED OPTICS 3301

A semi-analytical scheme to estimate Secchi-disk depth from Landsat-8 measurements

Zhongping Lee [a,*], Shaoling Shang [b,*], Lin Qi [a], Jing Yan [b], Gong Lin [b]

Remote Sensing of Environment 177 (2016) 101–106

Impact of sub-pixel variations on ocean color remote sensing products

Zhongping Lee,[1,*] Chuanmin Hu,[2] Robert Arnone,[3] and Zhen Liu[1]

10 September 2012 / Vol. 20, No. 19 / OPTICS EXPRESS 20844